



Minerva Access is the Institutional Repository of The University of Melbourne

Author/s:

Lidgerwood, GE;Senabouth, A;Smith-Anttila, CJA;Gnanasambandapillai, V;Kaczorowski, DC;Amann-Zalcenstein, D;Fletcher, EL;Naik, SH;Hewitt, AW;Powell, JE;Pébay, A

Title:

Transcriptomic Profiling of Human Pluripotent Stem Cell-derived Retinal Pigment Epithelium over Time

Date:

2021-04-01

Citation:

Lidgerwood, G. E., Senabouth, A., Smith-Anttila, C. J. A., Gnanasambandapillai, V., Kaczorowski, D. C., Amann-Zalcenstein, D., Fletcher, E. L., Naik, S. H., Hewitt, A. W., Powell, J. E. & Pébay, A. (2021). Transcriptomic Profiling of Human Pluripotent Stem Cell-derived Retinal Pigment Epithelium over Time. *Genomics Proteomics and Bioinformatics*, 19 (2), pp.223-242. <https://doi.org/10.1016/j.gpb.2020.08.002>.

Persistent Link:

<https://hdl.handle.net/11343/282508>

License:

[CC BY](#)



ORIGINAL RESEARCH

Transcriptomic Profiling of Human Pluripotent Stem Cell-derived Retinal Pigment Epithelium over Time

Grace E. Lidgerwood, Anne Senabouth, Casey J.A. Smith-Anttila, Vikkitharan Gnanasambandapillai, Dominik C. Kaczorowski, Daniela Amann-Zalcenstein, Erica L. Fletcher, Shalin H. Naik, Alex W. Hewitt, Joseph E. Powell, Alice Pébay

PII: S1672-0229(20)30135-2
DOI: <https://doi.org/10.1016/j.gpb.2020.08.002>
Reference: GPB 440

To appear in: *Genomics, Proteomics & Bioinformatics*

Received Date: 14 November 2019
Revised Date: 4 July 2020
Accepted Date: 9 August 2020

Please cite this article as: G.E. Lidgerwood, A. Senabouth, C.J.A. Smith-Anttila, V. Gnanasambandapillai, D.C. Kaczorowski, D. Amann-Zalcenstein, E.L. Fletcher, S.H. Naik, A.W. Hewitt, J.E. Powell, A. Pébay, Transcriptomic Profiling of Human Pluripotent Stem Cell-derived Retinal Pigment Epithelium over Time, *Genomics, Proteomics & Bioinformatics* (2020), doi: <https://doi.org/10.1016/j.gpb.2020.08.002>

This is a PDF file of an article that has undergone enhancements after acceptance, such as the addition of a cover page and metadata, and formatting for readability, but it is not yet the definitive version of record. This version will undergo additional copyediting, typesetting and review before it is published in its final form, but we are providing this version to give early visibility of the article. Please note that, during the production process, errors may be discovered which could affect the content, and all legal disclaimers that apply to the journal pertain.

1 **Transcriptomic Profiling of Human Pluripotent Stem Cell-derived**
2 **Retinal Pigment Epithelium over Time**

3 Grace E. Lidgerwood^{1,2,3,*}, Anne Senabouth⁴, Casey J.A. Smith-Anttila⁵, Vikkitharan
4 Gnanasambandapillai⁴, Dominik C. Kaczorowski⁴, Daniela Amann-Zalcenstein⁵, Erica L.
5 Fletcher¹, Shalin H. Naik^{5,6,7}, Alex W. Hewitt^{2,3,8,#}, Joseph E. Powell^{4,9,#}, Alice Pébay^{1,2,3,#,*}

6
7 ¹*Department of Anatomy and Neuroscience, The University of Melbourne, Parkville, VIC 3010,*
8 *Australia*

9 ²*Department of Surgery, The University of Melbourne, Parkville, VIC 3010, Australia*

10 ³*Centre for Eye Research Australia, Royal Victorian Eye and Ear Hospital, East Melbourne, VIC*
11 *3002, Australia*

12 ⁴*Garvan Weizmann Centre for Cellular Genomics, Garvan Institute of Medical Research, The*
13 *Kinghorn Cancer Centre, Darlinghurst, NSW 2010, Australia*

14 ⁵*Single Cell Open Research Endeavour, The Walter and Eliza Hall Institute of Medical Research,*
15 *Parkville, VIC 3052, Australia*

16 ⁶*Immunology Division, The Walter and Eliza Hall Institute of Medical Research, Parkville, VIC*
17 *3052, Australia*

18 ⁷*Department of Medical Biology, The University of Melbourne, Parkville, VIC 3010, Australia*

19 ⁸*School of Medicine, Menzies Institute for Medical Research, University of Tasmania, Hobart,*
20 *TAS 7005, Australia*

21 ⁹*UNSW Cellular Genomics Futures Institute, School of Medical Sciences, University of New South*
22 *Wales, Sydney, NSW 2052, Australia*

23

24 # Equal senior authors.

25 * Corresponding authors.

26 Email: grace.lidgerwood@unimelb.edu.au (Lidgerwood GE), apebay@unimelb.edu.au (Pébay A).

27

28 **Running Title:** *Lidgerwood GE et al / Temporal Transcriptomic Profiling of hPSC-derived RPE*

29

30 Total Words: 8203

31 References: 82

32 References from 2014: 42
33 Figures: 8
34 Tables: 0
35 Supplementary Figures: 4
36 Supplementary Tables: 7
37

Journal Pre-proofs

38 **Abstract**

39 Human pluripotent stem cell (hPSC)-derived progenies are immature versions of cells, presenting
40 a potential limitation to the accurate modelling of diseases associated with maturity or age. Hence,
41 it is important to characterise how closely cells used in culture resemble their native counterparts.
42 In order to select appropriate time points of retinal pigment epithelium (RPE) cultures that reflect
43 native counterparts, we characterised the transcriptomic profiles of the hPSC-derived RPE cells
44 from 1- and 12-month cultures. We differentiated the human embryonic stem cell line H9 into RPE
45 cells, performed single-cell RNA-sequencing of a total of 16,576 cells to assess the molecular
46 changes of the RPE cells across these two culture time points. Our results indicate the stability of
47 the RPE transcriptomic signature, with no evidence of an epithelial–mesenchymal transition, and
48 with the maturing populations of the RPE observed with time in culture. Assessment of Gene
49 Ontology pathways revealed that as the cultures age, RPE cells upregulate expression of genes
50 involved in metal binding and antioxidant functions. This might reflect an increased ability to
51 handle oxidative stress as cells mature. Comparison with native human RPE data confirms a
52 maturing transcriptional profile of RPE cells in culture. These results suggest that long-term *in*
53 *vitro* culture of RPE cells allows the modelling of specific phenotypes observed in native mature
54 tissues. Our work highlights the transcriptional landscape of hPSC-derived RPE cells as they age
55 in culture, which provides a reference for native and patient samples to be benchmarked against.

56

57 **KEYWORDS:** Human embryonic stem cell; Human pluripotent stem cell; Retinal pigment
58 epithelium; Single-cell RNA sequencing; Aging

59

60 **Introduction**

61 The retinal pigment epithelium (RPE) is a monolayer of post-mitotic, pigmented polarized cells
62 that is key to the health and function of photoreceptors and underlying vasculature. In particular,
63 the RPE protects the retina against photo-oxidation and phagocytoses photoreceptor outer
64 segments. The RPE is also essential to the immune privilege of the eye, as it physically contributes
65 to the blood–retina barrier and also expresses molecules repressing the migration of immune cells
66 into the retina [1]. In the human retina, aging is associated with vision decline and delayed dark
67 adaptation, both of which are direct consequences of tissue stress and retinal damage [2]. It is
68 hypothesized that over time, oxidative stress leads to the death of retinal neurons, a decrease in the
69 number of RPE cells, an accumulation of the toxic waste lipofuscin within the RPE, and an
70 accumulation of basal toxic deposits called drusen underneath the RPE [2]. Together, these events
71 contribute to a loss of homeostasis and low-grade inflammation within the retina [2]. Although it
72 is clear that the RPE is key to the health of the retina, the precise molecular mechanisms underlying
73 its aging are not well understood.

74 Human pluripotent stem cells (hPSCs) have the ability to propagate indefinitely *in vitro* and
75 give rise to any cell types in the body, including cells that form the retina. Various protocols have
76 been described to differentiate hPSCs into RPE cells [3–8]. RPE cells are generally assayed after
77 a few weeks of differentiation, at which stage they demonstrate similarity to their human native
78 counterparts, in terms of morphology/expression of key proteins, functions, and expression
79 profiles, however with a profile closer to a foetal stage than adult stage [4, 9, 10]. Interestingly,
80 the transcriptome profile of hPSC-derived RPE cells as they age in culture is unknown. To date,
81 most RNA-sequencing (RNA-seq) studies of RPE cells have been performed on bulk samples.
82 Yet, the ability to sequence individual cells provides a powerful tool to precisely uncover potential
83 heterogeneity in cell population, especially as these cells develop and mature *in vitro*. Here, we
84 used single-cell RNA-seq (scRNA-seq) of hPSC-derived RPE cells maintained in culture for 1
85 month or 12 months to assess the impact of time on the RPE transcriptome and whether genetic
86 hallmarks of maturation can be observed over time. A short-time differentiation (1 month) was
87 chosen as it represents a time point routinely used in *in vitro* assays of RPE [3]. A prolonged time
88 course of differentiation (12 months) was chosen as its characterization could be subsequently
89 used for comparison with other retinal cell differentiation methods, in particular of retinal

90 organoids and photoreceptors, for which differentiation and relative maturity are obtained after
91 prolonged time in culture and would thus be present at that later time point [11–14].

92

93 **Results**

94 **scRNA-seq profiles the transcriptomes of 16,576 cells**

95 The human embryonic stem cell (hESC) line H9 was differentiated to RPE cells following the
96 protocol described in the Materials and methods section. To generate a transcriptional map of the
97 RPE cells reflecting time in culture, RPE cells from the same culture and original passaging were
98 isolated after 1 month or 12 months of differentiation, dissociated to single cells, and processed to
99 generate libraries for scRNA-seq analysis (**Figure 1A**). The capture of single-cell library from the
100 1-month-old culture detected 12,873 cells at the mean read depth of 40,499 reads per cell, while
101 the capture from the 12-month-old culture detected 4850 cells at the mean read depth of 114,503
102 reads per cell (Table S1). Both datasets were subjected to cell-specific quality control, where 510
103 cells and 637 cells were removed from the 1-month-old and 12-month-old culture datasets,
104 respectively. The remaining 16,576 cells were retained for further analysis.

105 We compared variations in the transcriptomic profiles between the 1-month-old and 12-month-
106 old samples (Figure 1B and C) to identify potential changes in phenotypes upon aging of RPE cells
107 *in vitro*, by analysing differential expression. A range of RPE markers were observed as conserved
108 between both time points (Figure 1D). In particular, canonical RPE markers [15] associated with
109 extracellular structure organization (*CST3*, *EFEMP1*, *ITGAV*, *CRISPLD1*, and *ITGB8*), melanin
110 biosynthesis (*PMEL*, *TTR*, *TYRP1*, *TYR*, and *DCT*), lipid biosynthesis (*PTGDS* and *INPP5K*),
111 visual cycle (*LRAT*, *PLTP*, *ABHD2/RLBP1*, *RPE65*, *RGR*, *RBP1*, and *BEST1*), and secretion
112 (*SERPINF1*) were expressed at both time points (Figure 1D).

113

114 **Clustering analysis highlights 12 subpopulations of RPE cells**

115 Clustering analysis was performed independently for samples obtained at the two time points and
116 identified 12 subpopulations (clusters) in each sample (Figure 1C; Table S2). After integrating
117 with anchors identified with a method described previously [16], MetaNeighbor was used to match
118 common subpopulations across both samples [17], denoted as “Common”. Clusters unique to 1-
119 month-old and 12-month-old samples are denoted as “Young” and “Aged”, respectively (Figure
120 1C). In total, 18 subpopulations were identified, including six common subpopulations (Common

121 1–6; 8484 cells; Table S2), six subpopulations exclusive to the 1-month-old dataset (Young 0–5;
122 5758 cells; Table S2), and six subpopulations exclusive to the 12-month-old dataset (Aged 0–5;
123 2334 cells; Table S2). Cell counts per cluster (Figure 1C; Table S2) and the top conserved markers
124 for each distinct cluster (**Figure 2A**; Tables S3–S5) were identified. Clusters were visualised using
125 the Uniform Manifold Approximation and Projection (UMAP) plots (Figure 1B). In total, 3070
126 cells were considered singletons. These cells had fewer connections with similar cells (neighbors)
127 relative to the rest of the cell population and could not be assigned to a subpopulation. Cluster 0 in
128 the 1-month-old dataset (Young 0) comprises 2219 cells, accounting for 18% of all 1-month-old
129 cells, whereas Cluster 0 in the 12-month-old dataset (Aged 0) comprises 851 cells, accounting for
130 20% of all 12-month-old cells (Table S2). There were more singleton cells in the Young population
131 as we captured more cells from this group. We assessed the expression profile of genes
132 characteristic of progenitors (*BMP7* and *SOX4*) and canonical RPE genes [15] across all
133 subpopulations, both in terms of frequency and intensity of expression (Figure 2B; Tables S3–S5).
134 These genes are linked to lipid biosynthesis (*INPP5K* and *PTGDS*), visual cycle (*LRAT*, *RGR*,
135 *PLTP*, *RLBPI/CRALBP*, *RBPI/CRBPI*, *BEST1*, and *RPE65*), melanin biosynthesis (*DCT*, *TYRP1*,
136 *TYR*, *TTR*, and *PMEL*); secretion (*ENPP2*, *VEGFA*, and *SERPINF1*), phagocytic activity
137 (*GULP1*), and extracellular structure organization (*ITGAV*, *CRISPLD1*, *CST3*, and *EFEMP1*).
138 Most canonical RPE genes were expressed across most populations, although many were found at
139 lower levels in the 1-month-old cells, confirming the purity of the RPE cell cultures over time
140 (Figure 2B). As these transcripts are associated with stages of RPE maturity, our data indicate that
141 all subpopulations are of RPE lineage, potentially at various stages of differentiation and
142 maturation.

143

144 **Most cells share common transcriptomic profiles suggestive of maturing RPE cells**

145 We then performed differential gene expression analysis and pathway enrichment analysis to
146 characterise the molecular signature of these subpopulations. Of the cells examined, more than
147 half (8484 cells) were clustered into six Common subpopulations that intersect the 1-month-old
148 and 12-month-old cell cultures (Figure 1B and C), indicating a large shared transcriptional profile
149 between the two conditions. Some commonalities and differences were observed between the
150 Common samples arising from the 1-month-old and 12-month-old cultures. A range of RPE
151 markers was observed as conserved between samples collected at both time points (Figure 2B). In

152 particular, RPE markers associated with melanin biosynthesis (*MITF*, *PMEL*, *TTR*, *TYR*, *TYRPI*,
 153 and *DCT*), extracellular structure organization (*EFEMP1*, *CST3*, *CRISPLD1*, *ITGAV*, and *ITGB8*),
 154 secretion (*SERPINF1* and *VEGFA*), visual cycle (*RPE65*, *BEST1*, *RBP1*, *RLBP1*, *PLTP*, *RGR*, and
 155 *LRAT*), tight junctions (*TJPI*), phagocytic activity (*GULP1*), and lipid biosynthesis (*PTGDS*,
 156 *CYP27A1*, *INPP5K*, *PLA2G16*, and *PLCE1*) were conserved in all or some of the subpopulations
 157 (Table S3). Expression of some genes related to RPE maturity did not appear to differ between the
 158 1-month-old and 12-month-old RPE cells. These include *RBP1*, *TYRPI*, and *SERPINF1*,
 159 demonstrating that some genes encoding proteins necessary for retinoid-cycle binding, melanin
 160 biosynthesis and secretory are expressed in early RPE development (Figure 2B). More
 161 heterogeneity was observed in the expression of RPE markers *RGR*, *PLTP*, *RLBP1*, *BEST1*,
 162 *ENPP2*, *VEGFA*, and *TYR* in the 1-month-old RPE cells relative to the 12-month-old RPE cells,
 163 in which expression of these genes was generally high and stable (Figures 1D and 2B). Expression
 164 of *LRAT* and *RPE65* was predominantly observed in the 12-month-old RPE cells, with the
 165 exception of low expression of *RPE65* in the 1-month-old sample for the Common 2
 166 subpopulation. This suggests that the catabolic machinery converting all-*trans*-retinol into all-
 167 *trans*-retinyl ester (LRAT) and 11-*cis*-retinol (RPE65) for phototransduction is expressed at low
 168 levels in the 1-month-old RPE samples but becomes more comprehensive as cells age in culture
 169 (Figure 2C and D). Variations in the pattern of gene expression were observed between cells
 170 identified from the 1-month-old or 12-month-old cultures within each subpopulation (**Figure 3A–**
 171 **C**). Genes involved in neural differentiation, including *DCT*, *PAX6*, *SOX1*, and *MDK*, exhibited
 172 notable differences in expression between the 1-month-old and 12-month-old samples (Figure 3B).
 173 Similar patterns were also observed in genes involved in the extracellular matrix (ECM) formation
 174 and maintenance, including *CST3*, *EFEMP1*, *ITGAV*, and *CRISPLD1* (Figure 3C), which were
 175 more heterogeneous in the 1-month-old samples, suggesting transitional changes in ECM markers
 176 during early RPE differentiation. Examples of genes characteristics of RPE, neural differentiation,
 177 and ECM are illustrated in Figure 3A–C, respectively.

178 The common subpopulation 1 (Common 1, 2282 cells) was characterised by 891 conserved
 179 markers identified ($P < 0.74$) (Table S3). The most highly conserved markers include *NDUFA4L2*
 180 (a gene associated with the macula retina [18]), *CA9* (zinc metalloenzyme gene), as well as *DCT*,
 181 *PMEL*, *MITF*, *TYR*, and *TYRPI* (genes involved in pigment/melanin biosynthesis). This
 182 subpopulation also expressed genes involved in early retinal development including of the RPE

183 and eye morphogenesis (*SOX4*, *EFEMP1*, *BMP7*, *VIM*, *GJAI*, and *PTN*) and in the retinoid cycle
184 (*RPE65* and *RLBP1*). In addition, 79 ribosomal genes (32 *RPS* and 47 *RPL*) and 11
185 mitochondrially-encoded genes were identified. Expression of ribosomal genes and
186 mitochondrially-encoded genes has been correlated with development and maturation [19],
187 including of the retina [20, 21]. This is supported by the GO analysis showing an
188 overrepresentation of pathways involved in mitochondrial and ribosomal functions; protein
189 biogenesis, transport, assembly, and function; as well as ATP biosynthesis and metabolism (Figure
190 3D; Table S3). Hence, together with the presence of RPE markers, the data indicate this
191 subpopulation comprises a highly metabolically active maturing RPE phenotype.

192 The subpopulation Common 2 (2204 cells) identified 1077 conserved markers. The 15 most
193 conserved markers in this subpopulation were all known RPE markers. Many of the expressed
194 markers are involved in the generation of RPE cells or in maturation and homeostasis of these
195 cells. For instance, cystatin C encoded by *CST3* is abundantly produced by RPE cells [22] and its
196 secretion diminishes with age [23]. *DCT* is expressed in the developing retina [15] and is important
197 for melanin production and RPE homeostasis [24, 25]. Its downregulation is associated with
198 mature native RPE [26]. This demonstrates that this subpopulation is a mature functional RPE
199 population.

200 The subpopulation Common 3 (1811 cells) identified 1226 conserved markers. The most
201 conserved markers in this subpopulation were mostly known to be expressed in the RPE (*DCT*,
202 *TTR*, *CST3*, *AQP1*, *FTH1* [27], and *BEST1*), with some markers, such as *TFPI2*, known to promote
203 survival and maintenance of RPE cells [28]. The markers were similar to those of Common 2.
204 Other markers identified are not necessarily RPE-specific, e.g., *GNGT1* that encodes a protein
205 found in rod outer segments, suggesting that cells are not yet fully committed. Together, these
206 markers indicate cellular functions suggestive of functional and maturing RPE cells.

207 The subpopulation Common 4 (1170 cells) identified 1421 conserved markers. Many of the
208 most conserved markers of this subpopulation are not specifically linked to the RPE. For instance,
209 *TMSB4X* is linked to the cytoplasmic sequestering of NF- κ B but has not yet been reported to be
210 associated with molecular events in RPE cells. Many other genes are associated with the
211 cytoskeleton, such as *TAGLN*, *TNNC1*, *CALD1*, *MYLK*, *TPM1*, *ACTA2*, and *MYL9*. On the other
212 hand, there are many markers known to be expressed by the RPE cells, including *TTR*, *BEST1*,
213 *CST3*, *CSTV* [29], *CRYAB*, *SERPINF1*, *PMEL*, *VEGFA*, *RBPI*, *RLBP1*, *TYR*, and *TYRP1*,

214 supporting the RPE identity of this subpopulation. The presence of genes associated with early
215 differentiation, such as *IGFBP5* (downregulated relative to other clusters, as observed upon RPE
216 differentiation [30]) and *CRB2* [31], and genes involved in RPE polarity [32], is indicative of an
217 early stage of RPE maturity and of a differentiating RPE population.

218 The subpopulation Common 5 (630 cells; 907 conserved markers) was characterised by
219 expression of conserved RPE markers (*SERPINE2* [33], *SFRP5* [34]). Expression of many genes
220 (*AQP1*, *CST3*, *PTGDS*, *SERPINF1*, *BEST1*, and *SMOC2*) was downregulated when compared to
221 that in other populations. Expression patterns of other genes indicate an immaturity/ differentiation
222 or proliferation of cells, such as *GAP43*, *DAAMI*, *CD44* [35], and *DUSP4*. Together, these data
223 describe a subpopulation comprised of cells in early differentiation to RPE.

224 The subpopulation Common 6 (387 cells; 1664 conserved markers) was characterised by
225 markers associated with retinal cell types other than RPE [36] (such as *SPPI*, *CPODXL*, *STAC2*,
226 and *PCDH9*) or found at low levels in the RPE (such as *CPAMD8* and *SFRP2* [37]). Only the
227 marker *CRABP1* was highly conserved with expression upregulated, whilst expression of other
228 RPE markers (*SERPINF1*, *BEST1*, *RLBP1*, and *RPE65*) was downregulated. These data thus
229 suggest a subpopulation of immature cells.

230 Finally, the analysis of the PANTHER GO slim biological processes conserved within the
231 Common subpopulations identified pathways that are predominantly involved in mitochondrial,
232 metabolic, and ribosomal processes, as well as purine biosynthesis, nucleotide metabolism, protein
233 biogenesis, localisation, and transport (Figure 3D; Table S3). Altogether, these data demonstrate
234 that the population common to cultures at both time points is heterogeneous, with subpopulations
235 representing different stages of RPE cell differentiation.

236

237 **The Young subpopulations are characterised by immature and differentiating cells**

238 Around one third of all cells (5625 cells) were clustered into six Young subpopulations (Table S4).
239 Common RPE markers were conserved within several Young subpopulations (Figure 2A and B;
240 Table S4). These genes were associated with lipid biosynthesis (*PTGDS*), visual cycle (*RGR*,
241 *RLBP1*, *RBPI*, and *BEST1*), melanin biosynthesis (*DCT*, *TYRP1*, *TYR*, *TTR*, and *PMEL*),
242 phagocytic activity (*GULP1*), secretion (*ENPP2*, *VEGFA*, and *SERPINF1*), and extracellular
243 structure organisation (*ITGAV*, *CRISPLD1*, *CST3*, *EFEMP1*, and *ITGB8*).

244 The subpopulation Young 0 (2219 cells; 20 conserved markers) comprises singleton cells that
245 expressed *SERPINF1*, *CST3*, *DCT*, *TSC22D4*, *IGFBP5*, and *RNASE1*. Expression of most of these
246 genes has been reported in the retina (Courtesy of Human Protein Atlas, www.proteinatlas.org)
247 [36] and in the human RPE (*IGFBP5* [30]). PANTHER GO biological process analysis indicates
248 involvement of these genes in regulation of neuroblast proliferation, indicative of progenitor cells
249 (Table S4).

250 The subpopulation Young 1 (1873 cells; 58 conserved markers) was characterised by the
251 expression of *CTNNB1*, *NOG*, *ATP1B1*, *GSTP1*, *CD63*, and *HNRNPH1*. All these genes play
252 fundamental roles in the homeostasis and functions of the RPE. *ATP1B1* encodes an apical Na^+/K^+
253 ATPase, whose expression reduces with age and in age-related macular degeneration (AMD) [38].
254 Defects in *CTNNB1* are linked to abnormalities in RPE development and pigmentation [39],
255 whereas *GSTP1* is a survival factor for RPE cells, whose expression increases as cells mature [40];
256 *CD63* is a late endosome/exosome marker known to be released by RPE cells [41]; and *HNRNPH1*
257 levels are associated with improved survival of RPE cells in culture [42]. Hence, expression of
258 these markers indicates functional RPE cells. It is interesting to note that known canonical RPE
259 markers, such as *SERPINF1*, *RLBP1*, *TTR*, *PMEL*, and *CRYAB*, were expressed at lower levels in
260 this subpopulation than in all other subpopulations. GO biological process analysis highlights that
261 this population is highly metabolically active (Table S4). These data are suggestive of an earlier
262 stage of maturation of the RPE cells.

263 The subpopulation Young 2 (144 cells; 16 conserved markers) was characterised by the
264 specific upregulation of genes including *CCL2*, *SFRP1*, and *B2M*, downregulation of *CTSV* and
265 *TMSB4X*, as well as expression of *DCT*, which is known to be expressed during RPE development
266 [43], indicative of an immature RPE population.

267 The subpopulation Young 3 (67 cells; 369 conserved markers) was characterised by the
268 expression of genes such as *TOP2A*, *PCLAF*, *PTTG1*, *ANLN*, *MKI67*, *RRM2*, *TPX2*, and *PBK*.
269 Although all genes are found to be expressed in the retina [36], none are associated with a specific
270 RPE signature. However, these genes are associated with cell proliferation (*TOP2A*, *PCLAF*,
271 *PTTG1*, *MKI67*, *RRM2*, *TPX2*, and *PBK*) and cellular rearrangements (*ANLN*), which have been
272 described as characteristics of immature RPE cells [44]. In particular, *ANLN* is reported to promote
273 maturity of intercellular adhesions (tight junctions and adherens junctions) in epithelial cells [45].
274 *TOP2A* is associated with retinal development and proliferation [46], which, combined with

275 expression of *PCLAF*, *PTTG1*, and *MKI67*, suggests a proliferating cell population. Low
276 expression of RPE markers (*RBPI*, *ENPP2*, *CRABPI*, and *HNRNPFI*) further demonstrates the
277 RPE identity of the developing retinal cell subpopulation. Altogether, this expression profile
278 specifies an immature differentiating cell population.

279 The subpopulation Young 4 (871 cells; 49 conserved markers) was characterised by expression
280 of genes that are not traditionally associated with the RPE identity. The expression of *CRYAB*
281 (downregulated), *CRX*, *FTH1*, *TFPI2* (known to promote survival and maintenance of RPE cells
282 [28]), and *DCT* (expressed in the native RPE) suggests a differentiation to RPE, yet the presence
283 of the photoreceptor-specific *GNGT1* expression could also indicate an early differentiation step
284 where cells are not yet fully committed.

285 Interestingly, the subpopulation Young 5 (584 cells; 99 conserved markers) displayed a
286 signature comprising mitochondrial and ribosomal transcripts with 9 mitochondrial genes (MT-)
287 and 14 ribosomal genes (RPS- or RPL-). These genes are ubiquitous and have not been specifically
288 correlated to the retina or the RPE, however they are known to facilitate fundamental biological
289 processes, including electron transfer, energy provision, ribosome biogenesis, and protein
290 synthesis. PANTHER GO-slim biological process and GO biological process analyses confirmed
291 that the conserved pathways within this subpopulation are mostly related to the mitochondrial
292 energetic metabolism and nucleotide metabolism (Table S4). This subpopulation also expressed
293 RPE markers, such as *BEST1*, *VEGFA*, *ENPP2*, *TIMP3*, and *TYRPI*, as well as genes involved in
294 early retinal development including of the RPE and eye morphogenesis (*SOX11*, *PMEL*, *EFEMP1*,
295 *BMP7*, *VIM*, *GJA1*, and *PTN*) [15, 47]. Hence the presence of high level of expression of
296 mitochondrial genes and ribosomal genes in RPE is likely significative of highly active cells with
297 high levels of protein synthesis, implying that this is a maturing RPE population.

298 Taken together, our results demonstrate that all Young subpopulations are immature cells
299 developing to RPE cells.

300

301 **The Aged subpopulations are characterised by higher maturity of RPE cells**

302 Less than 10% of all cells (2334 cells) are clustered into the “Aged” category, which comprises
303 six subpopulations (Table S5). All six identified “Aged” subpopulations were subjected to the
304 same analysis as the “Young” and “Common” subpopulations. However, a statistical
305 overrepresentation test returned no positive results for subpopulations Aged 0, 1, and 5, most likely

306 owing to the low number of conserved genes identified. Only a few common RPE markers
 307 associated with lipid biosynthesis (*INPP5K*), visual cycle (*RLBP1*), melanin biosynthesis (*TTR*
 308 and *DCT*), secretion (*SERPINF1* and *VEGFA*), and extracellular structure organisation (*CST3* and
 309 *CRISPLD1*) were conserved in some of the “Aged” subpopulations (Figure 2; Table S5).

310 The subpopulation Aged 0 (851 cells; 6 conserved markers) is composed of singleton cells.
 311 These cells expressed *CRISPLD1*, *PCCA*, *WFDC1*, *TTR*, *SH3BGRL3*, and *TMSB4X*, but at lower
 312 average levels per cell than those in all other subpopulations. Some of these genes have been found
 313 to be expressed in the RPE (*CRISPLD1*, *WFDC1* [48], *TTR*, and *TMSB4X* [43]) and are associated
 314 with late RPE development (*CRISPLD1* and *TTR* [15]). Some other genes have a wider expression
 315 pattern (*PCCA* and *SH3BGRL3*) and encode for proteins involved in more universal cellular
 316 events. For instance, mitochondrial protein *PCCA* plays roles in death/survival, *SH3BGRL3* is
 317 involved in oxidoreduction, whilst *TMSB4X* encodes proteins of the cytoskeleton. Likewise, the
 318 subpopulation Aged 1 (815 cells; 12 conserved markers) presented more cells expressing
 319 *HSD17B2*, *TPM1*, *MYL9*, *NDUFA4L2*, *BNIP3*, *CALDI*, *TTR*, *DCT*, *MT-CYB*, *FTH1*, *CRYAB*, and
 320 *TMSB4X* but at lower average levels per cell than in all other subpopulations. Nine out of the
 321 twelve genes are known to be expressed in the RPE (*TTR*, *TMSB4X* [43], *CALDI* [49], *DCT* [43],
 322 *HSD17B2* [50], *NDUFA4L2* [15], *BNIP3* [27], *FTH1* [27], and *CRYAB*). Some of these markers
 323 are associated with late RPE development (*TTR* [15]), whilst others are associated with a
 324 geographic localisation of cells within the retina (*HSD17B2* [51] and *NDUFA4L2* [18]). *BNIP3*
 325 and *NDUFA4L2* encode for mitochondrial proteins playing roles in death/survival and electron
 326 transport, respectively, whilst *TPM1*, *MYL9*, *TMSB4X*, and *CALDI* encode proteins of the
 327 cytoskeleton. A similar pattern of expression was observed in the subpopulation Aged 5 (170 cells;
 328 6 conserved markers) with *PCCA*, *WFDC1*, *SERPINE2*, *TMSB4X*, and *TTR* being expressed in
 329 more cells with lower average levels than all other subpopulations. In addition, *SPON2*, which
 330 encodes ECM proteins important for cell adhesion, was expressed in more cells but at higher
 331 levels. The close similarities of these three Aged subpopulations point to a late RPE phenotype,
 332 with higher levels of maturation, towards regionalisation of cells.

333 Similarly, the subpopulations Aged 2 (46 cells; 22 conserved markers), Aged 3 (32 cells; 121
 334 conserved markers), and Aged 4 (420 cells; 34 conserved markers) showed close similarities in
 335 terms of gene expression profiles. The presence of known RPE markers, such as *DCT* (Aged 2,
 336 downregulated), *CALDI* (Aged 2, downregulated), *TTR* (Aged 3, downregulated; Aged 4), *SOX9*

337 (Aged 3, downregulated), *RBPI* (Aged 3, downregulated; Aged 4), *SERPINF1* (Aged 3,
338 downregulated), *VEGFA* (Aged 4, downregulated), *TMSB4X* (downregulated in all three
339 subpopulations), and *CRYAB* (downregulated in Aged 2 and Aged 3) confirms their RPE identity.

340 PANTHER GO-slim biological process (Aged 2) and PANTHER GO biological process
341 analyses (Aged 2, 3, and 4) were performed. Subpopulations Aged 2 and 4 were similar, with high
342 significance in pathways associated with response to metal ions (particularly cadmium, copper,
343 iron, and zinc); response to stress, chemicals, and toxins; and neural crest fate commitment.
344 Among them, neural crest fate commitment is the most significantly identified biological process
345 in Aged 3, with a 92.9-fold enrichment. Interestingly, GO analysis indicates that nuclear genes
346 encoding metallothioneins involved in metal binding (*MT1E*, *MT1F*, *MT1G*, *DCT*, *MT2A*), as well
347 as in oxidoreduction (*DCT*), were significantly differentially expressed between the “Aged”
348 subpopulations compared to all others, with an overall increased expression per cell as cells age
349 (Table S5). Further analysis of the metallothioneins *MT1E*, *MT1F*, *MT1G*, *MT1X*, and *MT2A*
350 across all subpopulations at the two time points confirms a large increase in their mRNA
351 expression in the 12-month-old culture when compared to the 1-month-old cells (**Figure 4A** and
352 **B**). On the other hand, expression of *DCT* was reduced in the 12-month-old culture compared to
353 the 1-month-old cells, which is consistent with a mature RPE profile [26] (Figure 4A and B).
354 Altogether, these data demonstrate that the RPE cells of these “Aged” subpopulations are
355 increasing their handling of metals and antioxidant abilities, which likely reflects a further
356 maturation of the RPE cells.

357

358 **RPE cells collected from different time points share common developmental trajectories**

359 We investigated the pseudo-temporal transition of 1-month-old cells to 12-month-old cells using
360 trajectory analysis methods to identify trajectories originating from proliferative cells in the
361 subpopulation Young 3. *Monocle 3* [52] identified a complex, branched development trajectory
362 that included cells from both time points (**Figure 5A** and **B**). Interestingly, the pseudo-temporal
363 ordering of cells across the trajectory did not correspond to time points (Figure S3A). To determine
364 the nature of the trajectories, we used Moran’s I test to identify 158 genes that were significantly
365 associated with pseudotime (Table S6). These genes formed four co-expression modules that were
366 further analysed with STRING (Table S6; Figure S3B–F). As illustrated in Figure S3, Module 1
367 revealed genes involved in development (red) and Module 4 revealed genes involved in cell cycle

368 (blue) and mitosis (red). The other two modules did not show clear biological process associations
369 but genes were associated with biological process for neural development. The differential
370 expression of the residual gene trajectory for the four modules confirms differences among various
371 clusters. In particular, all Young subpopulations except Young 4 showed the highest expression
372 levels of genes of the proliferative Module 4 (Figure S3B), confirming their immature proliferative
373 nature.

374 Differentiated RPE cells are post-mitotic and fully committed to the RPE lineage, in large part
375 due to their cell–cell contact inhibition [53, 54]. The expression of the proliferation marker *MKI67*
376 and of other genes associated with proliferation (*TOP2A*, *TPX2*, *PTTG1*, *PCLAF*, and *RRM2*) was
377 examined to assess whether some progenitor populations remain with proliferative potentials, and
378 whether these vary over time in culture. Our data indicate that only a small portion of cells
379 remained proliferative over time in culture. In particular, *MKI67* was almost uniquely expressed
380 in the immature subpopulation Young 3, together with other cell proliferation markers (*TOP2A*,
381 *TPX2*, *PTTG1*, *PCLAF*, and *RRM2*; Figure 5C; Table S4). Very few cells of the 12-month-old
382 population were found to express markers associated with proliferation (Figure 5C). This confirms
383 that only a small subpopulation of progenitor/immature cells present early in culture is proliferative
384 and these cells disappear with time in culture.

385 Pseudotime analyses of early retinal markers (*PAX6* and *RAX*) and RPE genes (*PMEL*, *RLPBI*,
386 *RGR*, *TYR*, *RBPI*, and *RPE65*) were performed in all subpopulations to measure gene expression
387 trajectories (Figure 5D and E; Figure S4). The early retinal markers *PAX* and *RAX*, were expressed
388 in similar manners across subpopulations, with minor variations between samples, with the
389 exception of the subpopulation Aged 3, which showed higher levels of *PAX6* and absence of
390 expression of *RAX* (Figure 5D and E; Figure S4). The pigmentation marker *TYR* was consistently
391 expressed across all populations, whilst expression of *PMEL* was downregulated in all aged
392 subpopulations and in subpopulations Common 5 and 6 (Figure 5D and E; Figure S4). Similarly,
393 comparable expression levels of *RGR*, *RLPBI*, and *RBPI* were observed across all subpopulations,
394 with the exception of subpopulations Aged 3 and 4, which showed higher levels of expression
395 (Figure 5D and E; Figure S4). These variations in gene expression are likely indicative of RPE cell
396 maturation in culture.

397

398 **RPE subpopulations contribute to paracrine signalling**

399 RPE cells can modulate immune responses and differentiation of other retinal cell types, in part
400 via paracrine signalling [1]. Such modulation can be detected *in vitro* through examining
401 expression of specific secretion factors and receptors known to play roles in immune or
402 developmental events. For instance, in the retina, the chemokine *CCL2* is implicated in monocyte
403 infiltration following damage [55] and its secretion by RPE cells contributes to the regulation of
404 the immunological response to inflammation [56]. *CCL2* was found to be faintly expressed in cells
405 at both time points (**Figure 6A**). *CCL2* was identified as a marker of the immature subpopulation
406 Young 2 (Table S2) and was also expressed, albeit at lower levels, across other “Aged” and
407 “Common” subpopulations (Figure 6A). Unsurprisingly, *CCR2*, which encodes the cognate
408 receptor of *CCL2*, was not expressed in any subpopulations, as it is most likely that *CCL2* targets
409 monocytes but not endogenous cells of the retina (data not shown). *CCL2* was more uniformly
410 expressed in the 12-month-old sample, suggesting more homogeneity in its expression as cells
411 mature.

412 Secreted frizzled-related proteins (SFRPs) are secreted ligands for receptors Frizzled (FZD1–
413 10), which are also receptors for WNT proteins (WNTs). Therefore, SFRPs are considered WNT
414 antagonists and can modulate WNT signalling. Cells in culture from both time points expressed
415 genes involved in the WNT signalling pathways, in particular *SFRP 1, 2, and 5*; *FZD 1 and 8*; as
416 well as *WNT 2B, 3, 4, and 5A*, with more expression homogeneity in the 12-month-old samples
417 for many of them (Figure 6B–J). *SFRP1* was expressed across all subpopulations with varied levels
418 and was identified as a marker of the immature subpopulation Young 2 (Figure 6B; Table S4).
419 *SFRP2* was identified as a marker of the immature subpopulation Common 6 where it was mainly
420 expressed, whilst *SFRP5* was identified as a marker of the immature subpopulation Common 5
421 and expressed across most subpopulations (Figure 6C and D; Table S3). It is interesting to note
422 that expression of *SFRP1* and *SFRP5* was both downregulated in the subpopulation Aged 3
423 (relative to other “Aged” subpopulations), reflective of a dynamic expression pattern of *SFRP*
424 genes by RPE cells in culture (Figure 6C and D; Table S3). Interestingly, 1-month-old RPE cells
425 showed low expression levels of *FZD1, FZD8, WNT2B, WNT3, WNT4, and WNT5A* with
426 expression of all other *FZD* and *WNT* genes undetectable (Figure 6E–J). The expression of all
427 detectible *SFRP, FZD, and WNT* genes was higher in the 12-month-old RPE cells (Figure 6B–J).
428 This dynamic profile of expression of molecules involved in WNT signalling indicates that RPE

429 cells can signal via the WNT pathway. This correlates with the known role of WNT signalling in
430 retinal development including the RPE [34, 57].

431 Pigment epithelium-derived factor (PEDF) is another factor key to various retinal cell
432 differentiation, maturation, and survival, including RPE and photoreceptors [58]. It is encoded by
433 *SERPINF1*, which is highly expressed by RPE cells and was found as a marker of subpopulations
434 within the Young, Common, and Aged subpopulations (Figure 1D; Tables S3–5). However, the
435 *PNPLA2*, the gene encoding PEDF receptor, was not found to be expressed in the RPE cells,
436 indicating that PEDF secreted from RPE largely acts in a paracrine manner. Likewise, *VEGFA*,
437 the gene encoding pleiotropic factor VEGF α [59], was also identified as a marker of
438 subpopulations within the three populations, but no expression of the gene encoding VEGF
439 receptor (*VEGFR1–3*) was detected in the samples, again indicating that the RPE-secreted VEGF
440 likely acts on neighbouring cells to maintain homeostasis (Figure 6K; Tables S3–S5). These
441 examples of paracrine molecules secreted by RPE subpopulations illustrate the important role
442 played by RPE cells in the shaping of a developing retina. These cells may release bioactive factors
443 to regulate events such as cell fate, differentiation, polarity, and maturity, and contribute to the
444 regulation of the immune environment of the retina.

445

446 ***APOE* is a conserved marker of various RPE subpopulations**

447 Apolipoproteins E (APOE) are proteins involved in lipid metabolism including cholesterol and are
448 also regulated with complement activation in the RPE [60]. APOEs interact with the low-density
449 lipoprotein (LDL) receptors (LDLRs) and very-low-density lipoprotein receptors (VLDLRs).
450 *APOE* was highly expressed in cells across both time points in culture (Figure 6L). *APOE* was
451 identified as a conserved marker of the subpopulations Young 1 and 5, as well as all Common
452 subpopulations (Figure 6L; Tables S3 and S4). The levels of *APOE* expression per cell was
453 however different between subpopulations, with an upregulation in Young 5, and a downregulation
454 in Young 1 as well as in Common 1, 2, 3, and 6 (Figure 6L). Interestingly, within the subpopulation
455 Common 4, cells arising from the 1-month-old culture expressed lower levels of *APOE* than cells
456 arising from 1-month-old culture of all other Common subpopulations, whereas the opposite was
457 observed for cells from 12-month-old culture (Table S3). The opposite pattern was observed in the
458 subpopulation Common 5 (Table S3). Expression of *LDLR*, *LRP1*, *LRP2*, and *LRP8*, the genes
459 encoding APOE receptors, was detected in both cell cultures, with increased levels in the 12-

460 month-old samples when compared to the 1-month-old culture (Figure 6M–P). Interestingly,
461 expression of these receptor genes was basically absent from all Young subpopulations, but present
462 at higher levels in the Aged subpopulations (Figure 6M–P). These data illustrate that the expression
463 of *APOE* and associated receptor genes is dynamic within RPE subpopulations and with time in
464 culture.

465

466 **The complement pathway is not modulated with time in culture**

467 RPE cells express many complement components in various retinal diseases, inflammation, and/or
468 aging [61]. *C1s*, *C1r*, and *CIQB*, the genes encoding complement regulators that form the C1
469 complex, were conserved markers in a few Young and Common subpopulations (Tables S3 and
470 S4). Other genes associated with the complement response (such as *CFH*, *CFB*, *CFHR1*, *CFHR3*,
471 and *C3*) were not identified as markers of any subpopulation (Tables S3–S5). This suggests that
472 the complement components are not modulated with time in culture.

473

474 **RPE cells do not undergo epithelial mesenchymal transition**

475 It is interesting to note that no markers of epithelial mesenchymal transition (such as *SNAIL*,
476 *SNAI2*, *ZEB1*, *TWIST1*, and *GSC*) were characterised in any examined subpopulation (Tables S3–
477 S5). These data demonstrate the stability of the cell culture over time, with no evidence of a
478 transition to a mesenchymal phenotype.

479

480 **RPE subpopulations express native RPE markers with different patterns**

481 To assess correspondence of the RPE cells with native counterparts, we compared the hPSC-
482 derived RPE signature to that of fetal native RPE cells, which was examined using scRNA-seq
483 previously [15]. As observed in fetal native tissue, most subpopulations of hPSC-derived RPE
484 cells expressed *SERPINF1*, *BEST1*, *TYR*, *TTR*, and *RPE65*, and the more immature subpopulations
485 also expressed *MKI67* and *DCT* (Figure 7A and B). Genes commonly expressed in native RPE
486 cells were enriched in 12-month-old subpopulations and in Aged subpopulations (such as *RPE65*,
487 *LRAT*, *PLTP*, *RGR*, *RLBP1*, *LRAT*, *INPP5K*, *ITGB8*, *EFEMP1*, *ITGAV*, *GULP1*, and *VEGFA*),
488 whilst other genes, including *TYRPI*, were found at similar expression levels in 1-month-old and
489 12-month-old cultures, as well as in Young, Common, and Aged populations (Figure 7C–H). In
490 addition, expression of some genes, such as *PMEL*, *PTGDS*, *CST3*, and *CRISPLD1*, was

491 significantly lower in 12-month-old cultures than that in 1-month-old cultures (Figure 7D–F).
492 Some common RPE genes are expressed in the adult native RPE at much higher levels than in fetal
493 RPE [26]. These include *TTR*, *RPE65*, *BEST1*, *CHRNA3*, *RBPI*, *MYRIP*, *TFPI2*, *PTGDS*,
494 *SERPINF1*, *DUSP4*, *GEM*, and *CRX*. Similarly, downregulation of *DCT*, *SFRP5*, *TYRP1*, and
495 *SLC6A15* is associated with mature native RPE [26]. We thus compared the expression profiles of
496 these genes in the RPE cultures over time, in order to assess the maturity of the cultured cells [26]
497 (**Figure 8**). *CHRNA3*, *MYRIP*, *GEM*, *CRX*, and *TFPI2* — whose expression is upregulated in the
498 adult native RPE— were more highly expressed in the Aged population (Figure 8A). However,
499 *PTGDS*, *RBPI*, and *DUSP4*, which are genes also highly expressed in the adult RPE, were not
500 found at higher levels in the Aged or 12-month-old cultures than in the Young population or 1-
501 month-old culture (Figures 7E and 8A). Expression of *DCT*, *PMEL*, *TYRP1*, *SFRP5*, and *SLC6A15*
502 was generally downregulated in the Aged subpopulations and in the 12-month-old Common
503 subpopulations, when compared to the 1-month-old Common subpopulations (Figure 7B and D;
504 Figure 8B).

505

506 Discussion

507 Here, we provide a dynamic profile of the transcriptome of hPSC-derived RPE cells over 12
508 months. Our data confirm expression of marker genes of RPE homeostasis and functions in hESC-
509 derived RPE [15, 26, 62, 63] and provide novel information on the timing of expression of these
510 markers. At both early and late time points, we observed that hPSC-derived RPE cells expressed
511 genes associated with lipid metabolism, secretion, visual cycle, melanin synthesis, phagocytic
512 activity, metal binding, and oxidoreductase activity. Based on expression pattern of genes
513 associated with RPE maturity levels and on PANTHER GO analyses, the 18 subpopulations
514 identified regroup into populations from immature and progenitor cells, to maturing RPE cells,
515 and functionally mature RPE cells (based on genes involved in RPE functions). Some
516 subpopulations comprised highly metabolically active cells. The pseudo-temporal analysis could
517 not identify trajectories matching time points, which is likely due to the experimental design of
518 including two time points only. Beyond the scope of this study but of interest, including
519 intermediate culture time points could provide more information on the pseudo-temporal ordering
520 of cells alongside the course of culture.

521 An essential function of the RPE is photoprotection of the retina, which is accomplished
522 through different mechanisms. These include absorbing radiation, binding and sequestering redox-
523 active metals such as iron, as well as scavenging free radicals and reactive oxygen species [64].
524 Metallothioneins are metal-binding proteins that are protective against oxidative stress. Compared
525 to the 12-month-old RPE cells, the 1-month-old RPE cells express fewer transcripts for the
526 metallothioneins *MT1E*, *MT1F*, *MT1G*, *MT2A*, and *MT1X*, as well as higher levels of *DCT*. These
527 data suggest a variation in the handling of metals and in the antioxidant abilities of RPE cells,
528 which could be reflective of either a necessity to handle more oxidative stress in an *in vitro* aging
529 environment or a maturation of RPE cells towards a more mature and protective phenotype [64].
530 The assessment of variations in the expression of other genes between the two time points indicates
531 a maturation profile of cells rather than an increased stress. Indeed, *DCT* is known to be expressed
532 in human retinal progenitor cells [15] and its expression is regulated by the early RPE marker
533 *MITF*. It is thus not surprising that as RPE cells mature, *MITF* expression reduces [65] and
534 subsequently *DCT* expression reduces, as is observed in human fetal retina [15]. Similarly,
535 *CTNNB1* regulates *MITF* and *OTX2* expression and subsequently RPE differentiation [39].
536 Finally, *SOX11* is known to be expressed in early retinal progenitor and early in differentiating
537 RPE cells [15, 47], hence its downregulation as cell culture ages further supports a maturation of
538 RPE cells in culture. The subpopulations Young 0 and Young 1 are characterised by the expression
539 of *CST3*, which encodes the cysteine proteinase inhibitor cystatin. Interestingly, this protein is
540 known to decrease in native RPE cells with aging [23]. Its presence in the cell population further
541 strengthens the implication of a maturing RPE population over time. The high expression levels
542 of mitochondrial and ribosomal genes in some cell populations likely indicate that cells are
543 metabolically and transcriptionally active, necessitating energy and ribosomal activities for protein
544 synthesis, respectively. It could also suggest that ribosomes potentially contribute to extra-
545 ribosomal functions in the RPE cells, such as cell development and maturation [19], as already
546 reported for melanocyte development [66], retinal development [20, 21], and retinal degeneration
547 [67]. Of note, the absence of markers of epithelial mesenchymal transition highlights the
548 robustness and ability of RPE cells to maintain their phenotype *in vitro* despite of prolonged culture
549 time.

550 The expression analysis of ligands and receptors involved in retinal development and
551 homeostasis demonstrates a dynamic profile of gene expression of hPSC-derived RPE cells. This

552 highlights the importance of the RPE in the development and homeostasis of the whole retina. For
553 instance, WNT signalling is important to the early stages of RPE differentiation [39, 68]. Some
554 *SFRPs* and *WNTs* are expressed in RPE cell subpopulations and the genes encoding FZD receptors
555 are very lowly expressed in most subpopulations. This suggests that the ligand expression could
556 be directed to paracrine signalling, playing roles in the development and homeostasis of other
557 neighbouring retinal cells. For instance, *SFRP 1, 2, and 5*, found to be expressed in the hPSC-
558 derived RPE cells, are associated with retinal development [34, 57], and known to promote the
559 differentiation of retinal ganglion cells and photoreceptors [69], and axon guidance [70]. Similarly,
560 high expression levels of *PEDF/SERPINF1* and of *VEGF* were found across many subpopulations,
561 yet genes encoding their respective receptors, *PNPLA2* and *VEGFR*, were not expressed in the
562 cells, suggestive of a paracrine signalling mechanism between RPE and neighbouring cells as well.
563 This is in accordance with the role of these growth factors in the biology and survival of retinal
564 cells, including photoreceptors [58, 71] and retinal ganglion cells [72], or beyond the retina in
565 neighbouring endothelial cells. Interestingly, *APOE* was also expressed in cells across both time
566 points in culture, with variations observed between subpopulations. In the RPE, APOE is involved
567 in lipid metabolism including cholesterol and drusen content [60]. APOE also plays a striking role
568 in melanogenesis, regulating the formation of functional premelanosome protein (PMEL) amyloid
569 fibrils in RPE cells [73]. Hence, the variations observed in its expression levels and that of its
570 receptors could possibly be indicators of melanogenesis within RPE subpopulations. Altogether,
571 the expression analysis of genes encoding ligands and receptors in RPE cells also hints at the
572 possible value of co-culturing RPE cells with retinal organoid cultures to further support retinal
573 differentiation and cell maturation, and to improve the *in vitro* modelling of retinal biology.

574 Our analyses also reveal that cells in culture can develop a transcriptomic profile more closely
575 related to the adult native RPE with higher expression levels of some RPE genes and lower
576 expression levels of others, as observed in their native counterpart. Altogether, these data thus
577 strongly suggest that as hPSC-derived RPE cells mature with time in culture, they acquire
578 characteristics more closely resembling those of an adult RPE profile.

579

580 **Conclusion**

581 The novel insight into the underlying genetic architecture of hPSC-derived RPE cells at short and
582 long durations in culture conditions reveals a gradual differentiation and maturation process, as

583 well as a stable RPE phenotype over time. Most cells with a clear RPE signature are found in the
584 Common subpopulations, indicating that RPE cells are present from an early time point in culture
585 and maintain this identity with time. The clustering analysis also reveals that whilst some
586 subpopulations express more genes associated with retinal and RPE biology, other RPE
587 subpopulations demonstrate increased expression in mitochondrial and/or ribosomal genes.
588 Altogether, these data suggest that hPSC-derived RPE cells develop their characteristic signatures
589 early during the differentiation process and continue to mature over time in culture. Our analysis
590 also warrants the use of hPSC-derived RPE cells for modelling of RPE biology at early and later
591 differentiation timings.

592

593 **Materials and methods**

594 **Cell culture and differentiation of hESCs to RPE cells**

595 The hESC line H9 (Wicell) was maintained on vitronectin-coated plates using StemFlex (Catalog
596 No. A3349401, Thermo Fisher Scientific, Waltham, MA), with medium changed every second
597 day [74]. Cells were differentiated into RPE cells as previously described [3] with the following
598 modifications. Briefly, hESCs were maintained in culture until reaching 70%–80% confluency, at
599 which stage StemFlex was replaced with Complete E6 (Catalog No. 05946, Stem Cell
600 Technologies, Vancouver, Canada) supplemented with N2 (Catalog No. 17502048, Thermo Fisher
601 Scientific) to induce retinal differentiation, with media changes 3 times/week for 33 days. On Day
602 33, medium was replaced with RPEM containing α -MEM (Catalog No. 12571071, Thermo Fisher
603 Scientific), 5% fetal bovine serum (Catalog No. 26140079, Thermo Fisher Scientific), non-
604 essential amino acids (Catalog No. 11140050, Thermo Fisher Scientific), penicillin- streptomycin-
605 glutamine (Catalog No. 10378016, Thermo Fisher Scientific), N1 (Catalog No. N6530, Sigma-
606 Aldrich, St Louis, MO), and taurine-hydrocortisone-triiodo-thyronin (in-house) to promote RPE
607 differentiation, with medium changed every second day. Cells were cultured for 32 days, a time
608 point at which maximal pigmentation is routinely observed. Cells were harvested with an 8-min
609 exposure to 0.25% trypsin-EDTA (Catalog No. 25200056, Thermo Fisher Scientific) and
610 inactivated with RPEM. Non-RPE contaminants (visible as unpigmented cells) were manually
611 removed from the culture, which begin shedding off the culture plate after \sim 2 min. Cells were
612 seeded at a density of 75,000 cells/cm² onto growth factor-reduced Matrigel-coated tissue culture
613 plates (Corning Matrigel hESC-qualified Matrix, Catalog No. 354277, *In vitro* Technologies,

614 Melbourne, Australia). Media was changed every second day, with the first sample of cells
615 harvested after 30 days (D30) and the second sample harvested on day 367 (D367) for scRNA-seq
616 analysis (Figure 1A).

617

618 **RPE cell harvest and single-cell preparation**

619 RPE cells were dissociated to single cells using 0.25% trypsin-EDTA for 8 min and inactivated
620 with RPEM. Cells were centrifuged at 300 g for 1 min to pellet and resuspended in a small volume
621 of RPEM containing 0.1% v/v propidium iodide (PI, Sigma-Aldrich) to exclude non-viable cells.
622 Single cell suspensions were passed through a 35- μ m filter prior to sorting. A minimum of 60,000
623 live cells (PI-negative) were sorted on a BD FACSAria IIu (100 μ m, 20 psi; BD-Biosciences, San
624 Jose, CA) into culture medium. Cells were centrifuged at 300 g for 5 min and resuspended in PBS
625 containing 0.04% BSA to a concentration of \sim 800–1000 cells/ μ l. Approximately 17,400 cells
626 were loaded onto a 10X chip for a target recovery of 10,000 cells. Cultures at the two time points
627 were captured separately to prepare two separate 10X reactions.

628

629 **Generation of single-cell gel beads in emulsion and sequencing libraries**

630 To generate single-cell gel beads in emulsion, single cell suspensions were loaded onto 10X
631 Genomics Single Cell 3' Chips together with the reverse transcription master mix following the
632 manufacturer's protocol for the Chromium Single Cell 3' v2 Library (PN-120233, 10X Genomics,
633 Pleasanton, CA). For each sample, sequencing libraries were generated with unique sample indices
634 (SI), assessed by gel electrophoresis (Agilent D1000 ScreenTape Assay, Santa Clara, CA) and
635 quantified with qPCR (Illumina KAPA Library Quantification Kit, Roche, Pleasanton, CA).
636 Following pooling and normalization to 4 nM, libraries were denatured and diluted to 1.6 pM for
637 loading onto the sequencer. Libraries were sequenced on an Illumina NextSeq 500 (NextSeq
638 Control Software v2.2.0 / Real Time Analysis v2.4.11) using NextSeq 500/550 High Output Kit
639 v2.5 (150 Cycles) (Catalog No. 20024907, Illumina, San Diego, CA) as follows: 26 bp (Read 1),
640 8 bp (i7 Index), and 98 bp (Read 2).

641

642 **Preprocessing, mapping, and quantification of scRNA-seq data**

643 We used the *cellranger mkfastq* and *cellranger count* pipelines from the Cell Ranger Single Cell
644 Software Suite (version 3.0.2) by 10x Genomics (<http://10xgenomics.com>) for initial quality

645 control, sample demultiplexing, mapping, and quantification of raw sequencing data. The
646 *cellranger count* pipeline was run with the following argument: “--expect-cells=10000”, and reads
647 were mapped to the *Homo sapiens* reference genome (GRCh38, Annotation: Gencode v29).
648 Filtered count matrices were then used for downstream analyses in R.

649

650 **Quality control and normalization**

651 Using Seurat v3.1.3 [16], data from the two culture time points underwent quality control and
652 normalization separately. The following values were calculated for each cell: total number of
653 unique molecular identifiers (UMIs), number of detected genes, as well as proportion of
654 mitochondrial and ribosomal transcripts relative to total expression. Cells were removed from
655 subsequent analysis if the total UMI count of the cell exceeded the threefold median absolute
656 deviation (MAD) across all cells in the sample. Manual thresholds were derived from outlier peaks
657 in the distributions of the number of detected genes, and fraction of mitochondrial and ribosomal
658 transcripts to total expression (Figure S1). Cells were removed from the 1-month time point sample
659 if the number of detected genes exceeded the lower and upper limits of 220 and 5000, respectively,
660 while cells from the 12-month time point sample were removed if the number of detected genes
661 was lower than 220. Cells from both time points were removed if mitochondrial transcripts
662 accounted for more than 25% of total expression, and/or ribosomal transcripts accounted for more
663 than 60% of total expression (Figure S1A–D; Table S1). The confounding effect of these
664 mitochondrial and ribosomal transcript QC metrics in remaining cells was regressed out during
665 cell–cell normalization, using the *SCTransform* function from Seurat [75] (Table S7).

666

667 **Integration, dimensionality reduction, and clustering**

668 Data dimensionality was reduced with principal component analysis (PCA). Subsequently, the 30
669 most statistically significant PCs were reduced to two dimensions using the Uniform Manifold
670 Approximation and Projection (UMAP) and used to construct a shared nearest neighbour (SNN)
671 graph for each cell. The Louvain method for community detection was then used to identify
672 clusters in each dataset with resolutions ranging from 0 to 1.5. The results for all resolutions were
673 plotted using *clustree* [76], which showed the stabilization of cell population identities at the
674 resolution of 0.6 in the 1-month culture and 0.7 in the 12-month culture (Figure S2A–C). Datasets
675 at both time points were combined into one dataset for comparative analysis with the integration

676 workflow from Seurat [77]. This workflow used canonical correlation analysis (CCA) to identify
677 22,023 anchors based on 3000 most variable genes. The anchors were then used to align both
678 datasets. To integrate the clusters across both time points, the unsupervised version of
679 MetaNeighbor [17] was used to evaluate the similarities between the 1-month clusters and 12-
680 month clusters. Cluster pairs that were reciprocally top hits and received a mean area under the
681 receiver operating characteristic (AUROC) score greater than 0.8 were merged into one cluster
682 (Figure S2D).

683

684 **Cluster characterization and analysis**

685 Network analysis was performed on differentially expressed genes (DEGs) using Reactome
686 functional interaction analysis [78, 79]. Differential expression (DE) analysis was performed using
687 the FindMarkers function based on the likelihood ratio test adapted for single-cell gene expression
688 [80]. GO analysis [81, 82] was performed using a PANTHER overrepresentation test [Fisher exact
689 test, false discovery rate (FDR) < 0.05] against the *Homo sapiens* genome (PANTHER version
690 14.1 released 2019-03-12). For some clusters, insufficient gene markers are available for GO
691 analysis (Aged Clusters 0, 1, and 5). Canonical RPE markers, gene expression profiles, and their
692 associated GO terms specific to each cluster are provided in Tables S3–S5.

693

694 **Trajectory analysis**

695 Trajectory analysis was performed with *Monocle 3* v0.2.4 [52]. Harmonized Pearson residuals
696 produced by the integration step underwent dimensionality reduction with UMAP, and the
697 resulting projection was used to initialize trajectory inference. The node closest to cells expressing
698 proliferative markers was selected as the root of the trajectory, and pseudotime values were
699 calculated. Gene expression dynamics across the trajectory was characterized with Moran I's test,
700 which was applied via the “*graph_test*” function using the following arguments: *neighbor_graph*
701 = “*principal_graph*”, *reduction_method* = “UMAP”, and *expression_family* = “*quasipoisson*”.
702 DEGs with $FDR \leq 0.05$ were clustered into co-expression modules using the “*find_gene_modules*”
703 function, and the resulting protein interactions were characterized with STRING.

704

705 **Ethical statement**

706 The experimental work was approved by the Human Research Ethics Committee of the University
707 of Melbourne (1545484), with the requirements of the National Health and Medical Research
708 Council (NHMRC) of Australia in accordance with the Declaration of Helsinki.

709

710 **Code availability**

711 Code and usage notes are available at:
712 https://github.com/powellgenomicslab/RPE_scRNA_AgedStudy. This repository consists of code
713 used to process raw sequencing data in FASTQ format to cell-gene expression tables via the Cell
714 Ranger pipeline, and code used to perform the following analyses: quality control, normalization,
715 dimensionality reduction, clustering, differential expression, and integration.

716

717 **Data availability**

718 Sequencing data are available at ArrayExpress (ArrayExpress: E-MTAB-8511). Files are raw
719 FASTQ files, and a tab separated matrix of UMIs per gene for each cell passing quality control
720 filtering. BAM files can be generated using the supplied repository to process the FASTQ files via
721 Cell Ranger.

722

723 **CRedit author statement**

724 **Grace E. Lidgerwood:** Conceptualization; Data curation; Formal analysis; Visualization;
725 Funding acquisition; Investigation; Methodology; Project administration; Resources;
726 Roles/Writing - original draft; Writing - review & editing. **Anne Senabouth:** Conceptualization;
727 Data curation; Formal analysis; Visualization; Methodology; Investigation; Software;
728 Roles/Writing - original draft; Writing - review & editing. **Casey J.A. Smith-Anttila,**
729 **Vikkitharan Gnanasambandapillai, Dominik C. Kaczorowski, Daniela Amann-Zalcenstein:**
730 Conceptualization; Methodology; Investigation; Roles/ Writing - review & editing. **Erica L.**
731 **Fletcher, Shalin H. Naik:** Conceptualization; Methodology; Funding acquisition; Roles/ Writing
732 - review & editing. **Alex W. Hewitt:** Conceptualization; Funding acquisition; Methodology;
733 Resources; Writing - review & editing, Supervision. **Joseph E. Powell:** Conceptualization; Data
734 curation; Formal analysis; Funding acquisition; Methodology; Resources; Software,
735 Roles/Writing - original draft; Writing - review & editing, Supervision. **Alice Pébay:**

736 Conceptualization; Formal analysis; Visualization; Funding acquisition; Methodology; Project
737 administration; Resources; Roles/Writing - original draft; Writing - review & editing, Supervision.
738 All authors read and approved the final manuscript.

739

740 **Competing interests**

741 The authors have declared no competing interests.

742

743 **Acknowledgments**

744 This work was supported by a National Health and Medical Research Council (NHMRC-
745 Australia) Practitioner Fellowship (awarded to AWH), Career Development Fellowship (awarded
746 to JEP), and Senior Research Fellowship (Grant No. 1154389, awarded to AP), an Australian
747 Research Council Future Fellowship (Grant No. FT140100047, awarded to AP), NHMRC project
748 grants (Grant Nos. 1138253 awarded to ELF and AP, as well as 1062820 and 1124812 awarded
749 to SHN), a NHMRC synergy grant (Grant No. 1181010 awarded to ELF and AP), grants from the
750 Macular Disease Foundation Australia (awarded to AP, JEP, and AWH), the Jack Brockhoff
751 Foundation (awarded to GEL), the DHB Foundation (awarded to GEL and AP), the Ophthalmic
752 Research Institute of Australia (awarded to AP and AWH), Stem Cells Australia – the Australian
753 Research Council Special Research Initiative in Stem Cell Science (awarded to SHN, AWH, JEP,
754 and AP), the TMG Family Fund (awarded to AP and GEL), a donation from Ms Jacqueline
755 Pascual, the University of Melbourne, and the Operational Infrastructure Support from the
756 Victorian Government, Australia.

757

758 **ORCID**

759 0000-0002-1774-5944 (Grace E. Lidgerwood)

760 0000-0002-8798-9821 (Anne Senabouth)

761 0000-0003-1391-7160 (Casey J.A. Smith-Anttila)

762 0000-0003-0306-1952 (Vikkitharan Gnanasambandapillai)

763 0000-0002-9205-1934 (Dominik C. Kaczorowski)

764 0000-0003-4928-1846 (Daniela Amann-Zalcenstein)

765 0000-0001-9412-9523 (Erica L. Fletcher)

766 0000-0003-0299-3301 (Shalin H. Naik)
767 0000-0002-5123-5999 (Alex W. Hewitt)
768 0000-0001-9031-6356 (Joseph E. Powell)
769 0000-0002-7408-9453 (Alice Pébay)

770

771 **References**

- 772 [1] Perez VL, Saeed AM, Tan Y, Urbieta M, Cruz-Guilloty F. The eye: a window to the soul of
773 the immune system. *J Autoimmun* 2013;45:7–14.
- 774 [2] Xu H, Chen M, Forrester JV. Para-inflammation in the aging retina. *Prog Retin Eye Res*
775 2009;28:348–68.
- 776 [3] Lidgerwood GE, Morris AJ, Conquest A, Daniszewski M, Rooney LA, Lim SY, et al. Role of
777 lysophosphatidic acid in the retinal pigment epithelium and photoreceptors. *Biochim*
778 *Biophys Acta Mol Cell Biol Lipids* 2018;1863:750–61.
- 779 [4] Lidgerwood GE, Lim SY, Crombie DE, Ali R, Gill KP, Hernández D, et al. Defined medium
780 conditions for the induction and expansion of human pluripotent stem cell-derived retinal
781 pigment epithelium. *Stem Cell Rev Rep* 2016;12:179–88.
- 782 [5] Kamao H, Mandai M, Okamoto S, Sakai N, Suga A, Sugita S, et al. Characterization of human
783 induced pluripotent stem cell-derived retinal pigment epithelium cell sheets aiming for
784 clinical application. *Stem Cell Rep* 2014;2:205–18.
- 785 [6] Osakada F, Jin Z-B, Hiramami Y, Ikeda H, Danjyo T, Watanabe K, et al. In vitro differentiation
786 of retinal cells from human pluripotent stem cells by small-molecule induction. *J Cell Sci*
787 2009;122:3169–79.
- 788 [7] Buchholz DE, Pennington BO, Croze RH, Hinman CR, Coffey PJ, Clegg DO. Rapid and
789 efficient directed differentiation of human pluripotent stem cells into retinal pigmented
790 epithelium. *Stem Cells Transl Med* 2013;2:384–93.
- 791 [8] Foltz LP, Clegg DO. Rapid, directed differentiation of retinal pigment epithelial cells from
792 human embryonic or induced pluripotent stem cells. *J Vis Exp* 2017:56274.
- 793 [9] Bennis A, Jacobs JG, Catsburg LAE, ten Brink JB, Koster C, Schlingemann RO, et al. Stem
794 cell derived retinal pigment epithelium: the role of pigmentation as maturation marker and
795 gene expression profile comparison with human endogenous retinal pigment epithelium.
796 *Stem Cell Rev Rep* 2017;13:659–69.
- 797 [10] Kokkinaki M, Sahibzada N, Golestaneh N. Human induced pluripotent stem-derived retinal
798 pigment epithelium (RPE) cells exhibit ion transport, membrane potential, polarized
799 vascular endothelial growth factor secretion, and gene expression pattern similar to native
800 RPE. *Stem Cells* 2011;29:825–35.
- 801 [11] Lidgerwood GE, Hewitt AW, Pébay A. Human pluripotent stem cells for the modelling of
802 diseases of the retina and optic nerve: toward a retina in a dish. *Curr Opin Pharmacol*
803 2019;48:114–9.

- 804 [12] Llonch S, Carido M, Ader M. Organoid technology for retinal repair. *Dev Biol* 2018;433:132–
805 43.
- 806 [13] Gagliardi G, Ben M'Barek K, Goureau O. Photoreceptor cell replacement in macular
807 degeneration and retinitis pigmentosa: A pluripotent stem cell-based approach. *Prog Retin*
808 *Eye Res* 2019;71:1–25.
- 809 [14] Sridhar A, Hoshino A, Finkbeiner CR, Chitsazan A, Dai L, Haugan AK, et al. Single-cell
810 transcriptomic comparison of human fetal retina, hPSC-derived retinal organoids, and long-
811 term retinal cultures. *Cell Rep* 2020;30:1644–59.e4.
- 812 [15] Hu Y, Wang X, Hu B, Mao Y, Chen Y, Yan L, et al. Dissecting the transcriptome landscape
813 of the human fetal neural retina and retinal pigment epithelium by single-cell RNA-seq
814 analysis. *PLoS Biol* 2019;17:e3000365.
- 815 [16] Stuart T, Butler A, Hoffman P, Hafemeister C, Papalexi E, Mauck WM 3rd, et al.
816 Comprehensive integration of single-cell data. *Cell* 2019;177:1888–902.e21.
- 817 [17] Crow M, Paul A, Ballouz S, Huang ZJ, Gillis J. Characterizing the replicability of cell types
818 defined by single cell RNA-sequencing data using MetaNeighbor. *Nat Commun* 2018;9:884.
- 819 [18] Tarau I-S, Berlin A, Curcio CA, Ach T. The cytoskeleton of the retinal pigment epithelium:
820 from normal aging to age-related macular degeneration. *Int J Mol Sci* 2019;20:3578.
- 821 [19] Zhou X, Liao W-J, Liao J-M, Liao P, Lu H. Ribosomal proteins: functions beyond the
822 ribosome. *J Mol Cell Biol* 2015;7:92.
- 823 [20] Barkić M, Crnomarković S, Grabusić K, Bogetić I, Panić L, Tamarut S, et al. The p53 tumor
824 suppressor causes congenital malformations in Rpl24-deficient mice and promotes their
825 survival. *Mol Cell Biol* 2009;29:2489–504.
- 826 [21] Watkins-Chow DE, Cooke J, Pidsley R, Edwards A, Slotkin R, Leeds KE, et al. Mutation of
827 the diamond-blackfan anemia gene *Rps7* in mouse results in morphological and
828 neuroanatomical phenotypes. *PLoS Genet* 2013;9:e1003094.
- 829 [22] Paraoan L, Grierson I, Maden BE. Analysis of expressed sequence tags of retinal pigment
830 epithelium: cystatin C is an abundant transcript. *Int J Biochem Cell Biol* 2000;32:417–26.
- 831 [23] Kay P, Yang YC, Hiscott P, Gray D, Maminishkis A, Paraoan L. Age-related changes of
832 cystatin C expression and polarized secretion by retinal pigment epithelium: potential age-
833 related macular degeneration links. *Invest Ophthalmol Vis Sci* 2014;55:926–34.
- 834 [24] Guyonneau L, Murisier F, Rossier A, Moulin A, Beermann F. Melanocytes and pigmentation
835 are affected in dopachrome tautomerase knockout mice. *Mol Cell Biol* 2004;24:3396–403.
- 836 [25] Takeda K, Yokoyama S, Yasumoto K-I, Saito H, Uono T, Takahashi K, et al. OTX2
837 regulates expression of DOPachrome tautomerase in human retinal pigment epithelium.
838 *Biochem Biophys Res Commun* 2003;300:908–14.
- 839 [26] Strunnikova NV, Maminishkis A, Barb JJ, Wang F, Zhi C, Sergeev Y, et al. Transcriptome
840 analysis and molecular signature of human retinal pigment epithelium. *Hum Mol Genet*
841 2010;19:2468–86.

- 842 [27] Strunnikova N, Zhang C, Teichberg D, Cousins SW, Baffi J, Becker KG, et al. Survival of
843 retinal pigment epithelium after exposure to prolonged oxidative injury: a detailed gene
844 expression and cellular analysis. *Invest Ophthalmol Vis Sci* 2004;45:3767–77.
- 845 [28] Tanaka Y, Utsumi J, Matsui M, Sudo T, Nakamura N, Mutoh M, et al. Purification, molecular
846 cloning, and expression of a novel growth-promoting factor for retinal pigment epithelial
847 cells, REF-1/TFPI-2. *Invest Ophthalmol Vis Sci* 2004;45:245–52.
- 848 [29] Alizadeh P, Smit-McBride Z, Oltjen SL, Hjelmeland LM. Regulation of cysteine cathepsin
849 expression by oxidative stress in the retinal pigment epithelium/choroid of the mouse. *Exp*
850 *Eye Res* 2006;83:679–87.
- 851 [30] Samuel W, Kutty RK, Vijayasarathy C, Pascual I, Duncan T, Redmond TM. Decreased
852 expression of insulin-like growth factor binding protein-5 during N-(4-
853 hydroxyphenyl)retinamide-induced neuronal differentiation of ARPE-19 human retinal
854 pigment epithelial cells: regulation by CCAAT/enhancer-binding protein. *J Cell Physiol*
855 2010;224:827–36.
- 856 [31] Quinn PM, Buck TM, Mulder AA, Ohonin C, Alves CH, Vos RM, et al. Human iPSC-derived
857 retinas recapitulate the fetal CRB1 CRB2 complex formation and demonstrate that
858 photoreceptors and Müller glia are targets of AAV5. *Stem Cell Rep* 2019;12:906–19.
- 859 [32] Paniagua AE, Herranz-Martín S, Jimeno D, Jimeno ÁM, López-Benito S, Carlos Arévalo J,
860 et al. CRB2 completes a fully expressed Crumbs complex in the retinal pigment epithelium.
861 *Sci Rep* 2015;5:14504.
- 862 [33] Winokur PN, Subramanian P, Bullock JL, Arocas V, Becerra SP. Comparison of two
863 neurotrophic serpins reveals a small fragment with cell survival activity. *Mol Vis*
864 2017;23:372–84.
- 865 [34] Chang JT, Esumi N, Moore K, Li Y, Zhang S, Chew C, et al. Cloning and characterization of
866 a secreted frizzled-related protein that is expressed by the retinal pigment epithelium. *Hum*
867 *Mol Genet* 1999;8:575–83.
- 868 [35] Liu NP, Roberts WL, Hale LP, Levesque MC, Patel DD, Lu CL, et al. Expression of CD44
869 and variant isoforms in cultured human retinal pigment epithelial cells. *Invest Ophthalmol*
870 *Vis Sci* 1997;38:2027–37.
- 871 [36] Uhlén M, Fagerberg L, Hallström BM, Lindskog C, Oksvold P, Mardinoglu A, et al.
872 Proteomics. Tissue-based map of the human proteome. *Science* 2015;347:1260419.
- 873 [37] Bennis A, Ten Brink JB, Moerland PD, Heine VM, Bergen AA. Comparative gene expression
874 study and pathway analysis of the human iris- and the retinal pigment epithelium. *PLoS One*
875 2017;12:e0182983.
- 876 [38] Cao L, Liu J, Pu J, Milne G, Chen M, Xu H, et al. Polarized retinal pigment epithelium
877 generates electrical signals that diminish with age and regulate retinal pathology. *J Cell Mol*
878 *Med* 2018;22:5552–64.
- 879 [39] Westenskow P, Piccolo S, Fuhrmann S. Beta-catenin controls differentiation of the retinal
880 pigment epithelium in the mouse optic cup by regulating *Mitf* and *Otx2* expression.
881 *Development* 2009;136:2505–10.

- 882 [40] Lee W-H, Joshi P, Wen R. Glutathione *S*-transferase pi isoform (GSTP1) expression in murine
883 retina increases with developmental maturity. *Adv Exp Med Biol* 2014;801:23–30.
- 884 [41] Wang AL, Lukas TJ, Yuan M, Du N, Tso MO, Neufeld AH. Autophagy and exosomes in the
885 aged retinal pigment epithelium: possible relevance to drusen formation and age-related
886 macular degeneration. *PLoS One* 2009;4:e4160.
- 887 [42] Pasovic L, Utheim TP, Reppe S, Khan AZ, Jackson CJ, Thiede B, et al. Improvement of
888 storage medium for cultured human retinal pigment epithelial cells using factorial design.
889 *Sci Rep* 2018;8:5688.
- 890 [43] Cai H, Shin MC, Tezel TH, Kaplan HJ, Del Priore LV. Use of iris pigment epithelium to
891 replace retinal pigment epithelium in age-related macular degeneration: a gene expression
892 analysis. *Arch Ophthalmol* 2006;124:1276–85.
- 893 [44] Alge CS, Suppmann S, Priglinger SG, Neubauer AS, May CA, Hauck S, et al. Comparative
894 proteome analysis of native differentiated and cultured dedifferentiated human RPE cells.
895 *Invest Ophthalmol Vis Sci* 2003;44:3629–41.
- 896 [45] Wang D, Chadha GK, Feygin A, Ivanov AI. F-actin binding protein, anillin, regulates
897 integrity of intercellular junctions in human epithelial cells. *Cell Mol Life Sci* 2015;72:3185–
898 200.
- 899 [46] Li Y, Hao H, Tzatzalos E, Lin R-K, Doh S, Liu LF, et al. Topoisomerase IIbeta is required
900 for proper retinal development and survival of postmitotic cells. *Biol Open* 2014;3:172–84.
- 901 [47] Usui A, Mochizuki Y, Iida A, Miyauchi E, Satoh S, Sock E, et al. The early retinal progenitor-
902 expressed gene *Sox11* regulates the timing of the differentiation of retinal cells. *Development*
903 2013;140:740–50.
- 904 [48] van Soest SS, de Wit GMJ, Essing AHW, ten Brink JB, Kamphuis W, de Jong PTVM, et al.
905 Comparison of human retinal pigment epithelium gene expression in macula and periphery
906 highlights potential topographic differences in Bruch's membrane. *Mol Vis* 2007;13:1608–
907 17.
- 908 [49] Tian J, Ishibashi K, Honda S, Boylan SA, Hjelmeland LM, Handa JT. The expression of
909 native and cultured human retinal pigment epithelial cells grown in different culture
910 conditions. *Br J Ophthalmol* 2005;89:1510–7.
- 911 [50] Whitmore SS, Wagner AH, DeLuca AP, Drack AV, Stone EM, Tucker BA, et al.
912 Transcriptomic analysis across nasal, temporal, and macular regions of human neural retina
913 and RPE/choroid by RNA-Seq. *Exp Eye Res* 2014;129:93–106.
- 914 [51] Cai H, Fields MA, Hoshino R, Del Priore LV. Effects of aging and anatomic location on gene
915 expression in human retina. *Front Aging Neurosci* 2012;4:8.
- 916 [52] Cao J, Spielmann M, Qiu X, Huang X, Ibrahim DM, Hill AJ, et al. The single-cell
917 transcriptional landscape of mammalian organogenesis. *Nature* 2019;566:496–502.
- 918 [53] Stern J, Temple S. Retinal pigment epithelial cell proliferation. *Exp Biol Med*
919 2015;240:1079–86.
- 920 [54] Qiu TG. Transplantation of human embryonic stem cell-derived retinal pigment epithelial
921 cells (MA09-hRPE) in macular degeneration. *NPJ Regen Med* 2019;4:19.

- 922 [55] Chen M, Forrester JV, Xu H. Dysregulation in retinal para-inflammation and age-related
923 retinal degeneration in CCL2 or CCR2 deficient mice. *PLoS One* 2011;6:e22818.
- 924 [56] Holtkamp GM, De Vos AF, Peek R, Kijlsta A. Analysis of the secretion pattern of monocyte
925 chemotactic protein-1 (MCP-1) and transforming growth factor-beta 2 (TGF-beta2) by
926 human retinal pigment epithelial cells. *Clin Exp Immunol* 1999;118:35–40.
- 927 [57] Bovolenta P, Esteve P, Ruiz JM, Cisneros E, Lopez-Rios J. Beyond Wnt inhibition: new
928 functions of secreted Frizzled-related proteins in development and disease. *J Cell Sci*
929 2008;121:737–46.
- 930 [58] He X, Cheng R, Benyajati S, Ma J-X. PEDF and its roles in physiological and pathological
931 conditions: implication in diabetic and hypoxia-induced angiogenic diseases. *Clin Sci*
932 2015;128:805–23.
- 933 [59] Penn JS, Madan A, Caldwell RB, Bartoli M, Caldwell RW, Hartnett ME. Vascular endothelial
934 growth factor in eye disease. *Prog Retin Eye Res* 2008;27:331–71.
- 935 [60] Yang P, Skiba NP, Tewkesbury GM, Treboschi VM, Baciú P, Jaffe GJ. Complement-
936 mediated regulation of Apolipoprotein E in cultured human RPE cells. *Invest Ophthalmol*
937 *Vis Sci* 2017;58:3073–85.
- 938 [61] Toomey CB, Johnson LV, Bowes Rickman C. Complement factor H in AMD: bridging
939 genetic associations and pathobiology. *Prog Retin Eye Res* 2018;62:38–57.
- 940 [62] Liao J-L, Yu J, Huang K, Hu J, Diemer T, Ma Z, et al. Molecular signature of primary retinal
941 pigment epithelium and stem-cell-derived RPE cells. *Hum Mol Genet* 2010;19:4229–38.
- 942 [63] May-Simera HL, Wan Q, Jha BS, Hartford J, Khristov V, Dejene R, et al. Primary cilium-
943 mediated retinal pigment epithelium maturation is disrupted in ciliopathy patient cells. *Cell*
944 *Rep* 2018;22:189–205.
- 945 [64] Rodríguez-Menéndez S, García M, Fernández B, Álvarez L, Fernández-Vega-Cueto A, Coca-
946 Prados M, et al. The Zinc-metallothionein redox system reduces oxidative stress in retinal
947 pigment epithelial cells. *Nutrients* 2018;10:1874.
- 948 [65] Capowski EE, Simonett JM, Clark EM, Wright LS, Howden SE, Wallace KA, et al. Loss of
949 *MITF* expression during human embryonic stem cell differentiation disrupts retinal pigment
950 epithelium development and optic vesicle cell proliferation. *Hum Mol Genet* 2014;23:6332–
951 44.
- 952 [66] McGowan KA, Li JZ, Park CY, Beaudry V, Tabor HK, Sabnis AJ, et al. Ribosomal mutations
953 cause p53-mediated dark skin and pleiotropic effects. *Nat Genet* 2008;40:963–70.
- 954 [67] Grewal R, Stepczynski J, Kelln R, Erickson T, Darrow R, Barsalou L, et al. Coordinated
955 changes in classes of ribosomal protein gene expression is associated with light-induced
956 retinal degeneration. *Invest Ophthalmol Vis Sci* 2004;45:3885–95.
- 957 [68] Leach LL, Buchholz DE, Nadar VP, Lowenstein SE, Clegg DO. Canonical/ β -catenin Wnt
958 pathway activation improves retinal pigmented epithelium derivation from human
959 embryonic stem cells. *Invest Ophthalmol Vis Sci* 2015;56:1002–13.
- 960 [69] Esteve P, Trousse F, Rodríguez J, Bovolenta P. SFRP1 modulates retina cell differentiation
961 through a beta-catenin-independent mechanism. *J Cell Sci* 2003;116:2471–81.

- 962 [70] Rodriguez J, Esteve P, Weinl C, Ruiz JM, Fermin Y, Trousse F, et al. SFRP1 regulates the
 963 growth of retinal ganglion cell axons through the Fz2 receptor. *Nat Neurosci* 2005;8:1301–
 964 9.
- 965 [71] Saint-Geniez M, Maharaj ASR, Walshe TE, Tucker BA, Sekiyama E, Kurihara T, et al.
 966 Endogenous VEGF is required for visual function: evidence for a survival role on Müller
 967 cells and photoreceptors. *PLoS One* 2008;3:e3554.
- 968 [72] Nishijima K, Ng Y-S, Zhong L, Bradley J, Schubert W, Jo N, et al. Vascular endothelial
 969 growth factor-A is a survival factor for retinal neurons and a critical neuroprotectant during
 970 the adaptive response to ischemic injury. *Am J Pathol* 2007;171:53–67.
- 971 [73] van Niel G, Bergam P, Di Cicco A, Hurbain I, Lo Cicero A, Dingli F, et al. Apolipoprotein E
 972 regulates amyloid formation within endosomes of pigment cells. *Cell Rep* 2015;13:43–51.
- 973 [74] Daniszewski M, Nguyen Q, Chy HS, Singh V, Crombie DE, Kulkarni T, et al. Single-cell
 974 profiling identifies key pathways expressed by iPSCs cultured in different commercial
 975 media. *iScience* 2018;7:30–9.
- 976 [75] Hafemeister C, Satija R. Normalization and variance stabilization of single-cell RNA-seq data
 977 using regularized negative binomial regression. *Genome Biol* 2019;20:296.
- 978 [76] Zappia L, Oshlack A. Clustering trees: a visualization for evaluating clusterings at multiple
 979 resolutions. *Gigascience* 2018;7:giy083.
- 980 [77] Butler A, Hoffman P, Smibert P, Papalexi E, Satija R. Integrating single-cell transcriptomic
 981 data across different conditions, technologies, and species. *Nat Biotechnol* 2018;36:411–20.
- 982 [78] Anders S, Huber W. Differential expression analysis for sequence count data. *Genome Biol*
 983 2010;11:R106.
- 984 [79] Wu G, Feng X, Stein L. A human functional protein interaction network and its application
 985 to cancer data analysis. *Genome Biol* 2010;11:R53.
- 986 [80] McDavid A, Finak G, Chattopadhyay PK, Dominguez M, Lamoreaux L, Ma SS, et al. Data
 987 exploration, quality control and testing in single-cell qPCR-based gene expression
 988 experiments. *Bioinformatics* 2013;29:461–7.
- 989 [81] Ashburner M, Ball CA, Blake JA, Botstein D, Butler H, Cherry JM, et al. Gene ontology: tool
 990 for the unification of biology. The Gene Ontology Consortium. *Nat Genet* 2000;25:25–9.
- 991 [82] The Gene Ontology Consortium. The Gene Ontology resource: 20 years and still going
 992 strong. *Nucleic Acids Res* 2019;47:D330–8.

993

994 **Figure legends**

995 **Figure 1** scRNA-seq transcriptome profiling of hPSC-derived RPE cells reveals 18
 996 subpopulations

997 **A.** Schematic representations of the experimental flow. **B.** UMAP of single-cell expression profile
 998 from 16,576 cells, clustered into 18 subpopulations, split by condition (1-month-old and 12-month-
 999 old) and combined. **C.** Cluster grouping represented by a Venn diagram, identifying 18

1000 subpopulations, showing Young (red), Aged (green), and their common subpopulations (blue).
 1001 Number of cells for each subpopulation is indicated in bold below the subpopulation name. **D.**
 1002 UMAP of canonical RPE markers in 1-month-old and 12-month-old cultures, organised by cellular
 1003 functions: extracellular structure organization (*CST3*, *EFEMP1*, *ITGAV*, *CRISPLD1*, and *ITGB8*);
 1004 melanin biosynthesis (*PMEL*, *TTR*, *TYRP1*, *TYR*, and *DCT*), lipid biosynthesis (*PTGDS* and
 1005 *INPP5K*), visual cycle (*LRAT*, *PLTP*, *RLBP1*, *RPE65*, *RGR*, *RBPI*, and *BEST1*), as well as
 1006 secretion (*SERPINF1*). Levels of gene expression per cell (percentage expressed) are shown with
 1007 colour gradients. scRNA-seq, single-cell RNA sequencing; hPSC, human pluripotent stem cell;
 1008 RPE, retinal pigment epithelium; UMAP, Uniform Manifold Approximation and Projection for
 1009 Dimension Reduction.

1010

1011 **Figure 2 Characterisation of hPSC-derived RPE populations**

1012 **A.** Heatmap showing the most conserved markers (gene symbols are indicated on the left side) in
 1013 all individual cells in each of the 18 subpopulations (indicated on top, with colours matching those
 1014 of subpopulations shown in Figure 1C). Gene expression levels were scaled and presented as
 1015 average of Log₂-transformed FC. **B.** Dotplot representation of single-cell expression profile from
 1016 1-month-old and 12-month-old cells for selected gene markers, representative of progenitor cells,
 1017 or RPE with genes linked to RPE functions. Populations arising from 1-month-old cultures are
 1018 represented in orange and those from 12-month-old cultures in black. Levels of gene expression
 1019 per cell are shown with colour gradients, and frequencies of cells expressing the respective gene
 1020 (percentage expressed) are shown with size of dots. RPE markers are coloured according to their
 1021 cellular functions. FC, fold change.

1022

1023 **Figure 3 Expression patterns of selected conserved markers and GO pathway in the hPSC-** 1024 **derived RPE cells**

1025 Expression values are measured as normalised UMI counts. **A.** Violin plot of selected conserved
 1026 markers in each Common subpopulation characteristic of the RPE. **B.** Violin plot of selected
 1027 conserved markers in each Common subpopulation characteristic of the neural differentiation. **C.**
 1028 Violin plot of selected conserved markers in each Common subpopulation characteristic of the
 1029 ECM. The plots describe the distribution and relative expression of each transcript in each common
 1030 subpopulation, with separation of cells belonging to the 1-month-old (blue) and 12-month-old

1031 (brown) cultures. **D.** PANTHER GO-slim (biological process) pathways associated with each of
1032 the Common subpopulations (Common 1–6; colour-coded) identified via over-representation
1033 analysis. Association is measured by fold enrichment, that is calculated from the number of genes
1034 observed, divided by the expected number of genes to be present by chance. UMI, unique
1035 molecular identifier; ECM, extracellular matrix.

1036

1037 **Figure 4 Aged RPE subpopulations likely increase their handling of metals and antioxidant**
1038 **abilities**

1039 **A.** Feature plots of expression profiles of *DCT* and genes encoding key metallothioneins (including
1040 *MT1E*, *MT1F*, *MT1G*, *MT1X*, and *MT2A*) across the 1-month-old and 12-month-old cells. The
1041 intensity of gene expression is indicated by colour gradient. **B.** Ridge plots of expression profiles
1042 (measured in natural log-normalised UMI counts) of *DCT* and genes encoding key
1043 metallothioneins and across all subpopulations. Different colours are used for each subpopulation
1044 for ease of reading.

1045

1046 **Figure 5 Only a few cells retain a proliferative profile**

1047 Highly dimensional expression data were reduced into two dimensions using UMAP. Plot axes
1048 (UMAP1 and UMAP2) represent coordinates in the resulting 2D space. **A.** UMAP of single cell
1049 expression profile split by conditions (1-month-old and 12-month-old). **B.** UMAP of single cell
1050 expression profile for trajectory analysis using Monocle 3. **C.** UMAP of single cell expression
1051 profile for markers associated with proliferation (*MKI67*, *TOP2A*, *PCLAF*, *RRM2*, *TPX2*, and
1052 *PTTGI*) across all cells. Expression levels measured as Log_{10} normalized UMI counts are
1053 represented by colour intensity. Lines represent differentiation trajectories as calculated by
1054 Monocle3. **D.** Pseudotime analysis of early retinal markers (*PAX6* and *RAX*) and RPE genes
1055 (*PMEL*, *RLBP1*, *RGR*, *TYR*, *RBPI*, and *RPE65*) across the 1-month-old and 12-month-old cells.
1056 Expression levels measured as Log_{10} normalized UMI counts are represented by colour intensity.
1057 Lines represent differentiation trajectories as calculated by Monocle3. **E.** Violin plots of
1058 normalised UMI counts of early retinal markers and RPE genes across all subpopulations showing
1059 variations in expression across cluster groups.

1060

1061 **Figure 6 RPE subpopulations contribute to paracrine signalling**

1062 UMAP of single-cell expression profile of markers for 1-month-old and 12-month-old cultures,
 1063 with associated violin plots , representing Log₂ UMI counts across all populations for *CCL2* (A);
 1064 *SFRPs*, *FZDs*, and *WNTs* (B); *VEGFA* (C); *APOE*, *LDLR*, and *LRPs* (D). In the UMAPs, the
 1065 intensity of gene expression is indicated by colour gradient. UMAP of single-cell expression
 1066 profile of markers for 1-month-old and 12-month-old cultures, with associated violin plots across
 1067 all populations for *CCL2* (A), *SFRP1* (B), *SFRP2* (C), *SFRP5* (D), *FZD1* (E), *FZD8* (F), *WNT2B*
 1068 (G), *WNT3* (H), *WNT4* (I), *WNT5A* (J), *VEGFA* (K), *APOE* (L), *LDLR* (M), *LRP1* (N), *LRP2* (O),
 1069 *LRP8* (P). In the UMAP plots, the intensity of gene expression is indicated by colour gradient. In
 1070 the violin plots, different colours are used for each subpopulation for ease of reading.

1071

1072 **Figure 7 hPSC-derived RPE subpopulations express native RPE markers with different**
 1073 **patterns**

1074 Violin plots of selected markers representative of native RPE cells (obtained from [28]) across all
 1075 subpopulations and in the three main populations “Young”, “Aged”, “Common”, represented in
 1076 different colours. Subpopulations arising from the 1-month-old culture are indicated in yellow;
 1077 subpopulations arising from the 12-month-old culture are indicated in blue. **A.** Genes found in all
 1078 subpopulations (*SERPINF1*, *BEST1*, *TYR*, *TTR*, and *RPE65*). **B.** Genes found in more immature
 1079 subpopulations (*SFRP2*, *MKI67*, and *DCT*). **C.** Genes with varied expression associated with
 1080 visual cycle (*PLTP*, *RGR*, *RLBP1*, and *LRAT*). **D.** Genes with varied expression associated with
 1081 melanin biosynthesis (*PMEL* and *TYRP1*). **E.** Genes with varied expression associated with lipid
 1082 biosynthesis (*PTGDS* and *INPP5K*). **F.** Genes with varied expression associated with extracellular
 1083 structure organisation (*CST3*, *ITGB8*, *EFEMP1*, *ITGAV*, and *CRISPLD1*). **G.** Genes with varied
 1084 expression associated with phagocytic activity (*GULP1*). **H.** Genes with varied expression
 1085 associated with secretion (*VEGFA*). The plots describe the distribution and relative expression of
 1086 each gene in the subpopulations, measured as normalised UMI counts.

1087

1088 **Figure 8 Some hPSC-derived RPE subpopulations acquire a gene expression profile closer**
 1089 **to adult native RPE with time in culture**

1090 Violin plots of selected markers representative of native adult RPE cells (obtained from [28])
 1091 across all subpopulations and in the three main populations “Young”, “Aged”, “Common”,
 1092 represented in different colours. Subpopulations arising from the 1-month-old culture are indicated

1093 in yellow; subpopulations arising from the 12-month-old culture are indicated in blue. **A.** Genes
1094 with upregulated expression in adult RPE (*CHRNA3*, *RBPI*, *MYRIP*, *DUSP4*, *GEM*, *CRX*, and
1095 *TFPI2*). **B.** Genes with downregulated expression in adult RPE (*SFRP5* and *SLC6A15*). The plots
1096 describe the distribution and relative expression of each gene in the subpopulations, measured as
1097 normalised UMI counts.

1098

1099 **Supplementary materials**

1100 **Figure S1 Filtering of cells based on quality control metrics**

1101 **A.** Total number of UMIs per cell. **B.** Total number of features per cell. **C.** Percentage of
1102 mitochondrial gene expression relative to total expression. **D.** Percentage of ribosomal gene
1103 expression relative to total expression. **E.** Relationship between total UMIs, detected genes, and
1104 percentage of mitochondrial gene expression. Histograms for total UMIs and detected features are
1105 located on X and Y margins of scatter plot, respectively. Scatter plot represents the relationships
1106 between the two metrics and are coloured by percentage of mitochondrial expression. Plots for 1-
1107 month-old culture and 12-month-old culture are shown on the left and right, respectively. UMI,
1108 unique molecular identifier; MAD, median absolute deviation.

1109

1110 **Figure S2 Characterisation of stable cell subpopulations**

1111 Graph-based clustering was performed at different resolutions ranging from 0 to 1.5, in increments
1112 of 0.1 for 1-month-old (**A**), 12-month-old (**B**), and combined (**C**) datasets using *clustree*. Regions
1113 of stability are represented by minimal branching. Values within circles are arbitrary cluster
1114 identifiers and arrows indicate the proportion of cells moving from one group to another
1115 (transitioning cells, colour coded). **D.** Integration of clusters identified in 1-month-old and 12-
1116 month-old cells via MetaNeighbor. Heatmap represents degree of similarity of clusters as AUROC
1117 values. AUROC, area under receiver operating characteristic curve.

1118

1119 **Figure S3 Residual trajectory genes modules analyses measured with Monocle 3**

1120 **A.** Monocle 3 pseudotime represented in beeswarm plots. Different colours are used for each
1121 subpopulation for ease of reading. **B.** Heatmap of module scores for each subpopulation. Modules
1122 were identified via Monocle 3 gene trajectory analysis, and module scores were calculated via
1123 differential expression of genes from each module. **C.** STRING analysis of genes from Table S6

1124 for Module 1. Genes involved in regulation of development are shown in red. **D.** STRING analysis
1125 of genes from Table S6 for Module 2. Genes involved in regulation of synapse organisation are
1126 shown in red. **E.** STRING analysis of genes from Table S6 for Module 3. No relevant biological
1127 processes was revealed. **F.** STRING analysis of genes from Table S6 for Module 4. Genes
1128 involved in regulation of cell cycle and mitosis are shown in blue and red, respectively.

1129

1130 **Figure S4 Gene trajectory by pseudotime analyses of early and mature RPE markers**

1131 Gene expression (measured as normalised UMI count) of early (*MITF*, *PAX6*, *PMEL*, *RAX*, and
1132 *SIX3*) and mature RPE markers (*RBPI*, *RGR*, *RLBPI*, *RPE65*, and *TYR*) using Monocle 3, with
1133 each subpopulation coded in colour as indicated. Trend of expression is represented by a black line
1134 within each panel.

1135

1136 **Table S1 Quality control parameters**

1137

1138 **Table S2 Cluster analysis with number of cells per subpopulation**

1139

1140 **Table S3 Conserved cluster markers, PANTHER Gene Ontology pathways and differential 1141 expression for each subpopulation within the “Common” population**

1142

1143 **Table S4 Conserved cluster markers and Gene Ontology pathways for each subpopulation 1144 within the “Young” population**

1145

1146 **Table S5 Conserved cluster markers and Gene Ontology pathways for each subpopulation 1147 within the “Aged” population**

1148

1149 **Table S6 Monocle3 residual trajectory**

1150 **Table S7 Details of cell filtration criteria.**

1151

1152 **Authors' contributions**

1153 Grace E. Lidgerwood: Conceptualization; Data curation; Formal analysis; Visualization; Funding
1154 acquisition; Investigation; Methodology; Project administration; Resources; Roles/Writing -
1155 original draft; Writing - review & editing.

1156 Anne Senabouth: Conceptualization; Data curation; Formal analysis; Visualization; Methodology;
1157 Investigation; Software; Roles/Writing - original draft; Writing - review & editing.

1158 Casey J.A. Smith-Anttila, Vikkitharan Gnanasambandapillai, Dominik C. Kaczorowski, Daniela
1159 Amann-Zalcenstein: Conceptualization; Methodology; Investigation; Roles/ Writing - review &
1160 editing.

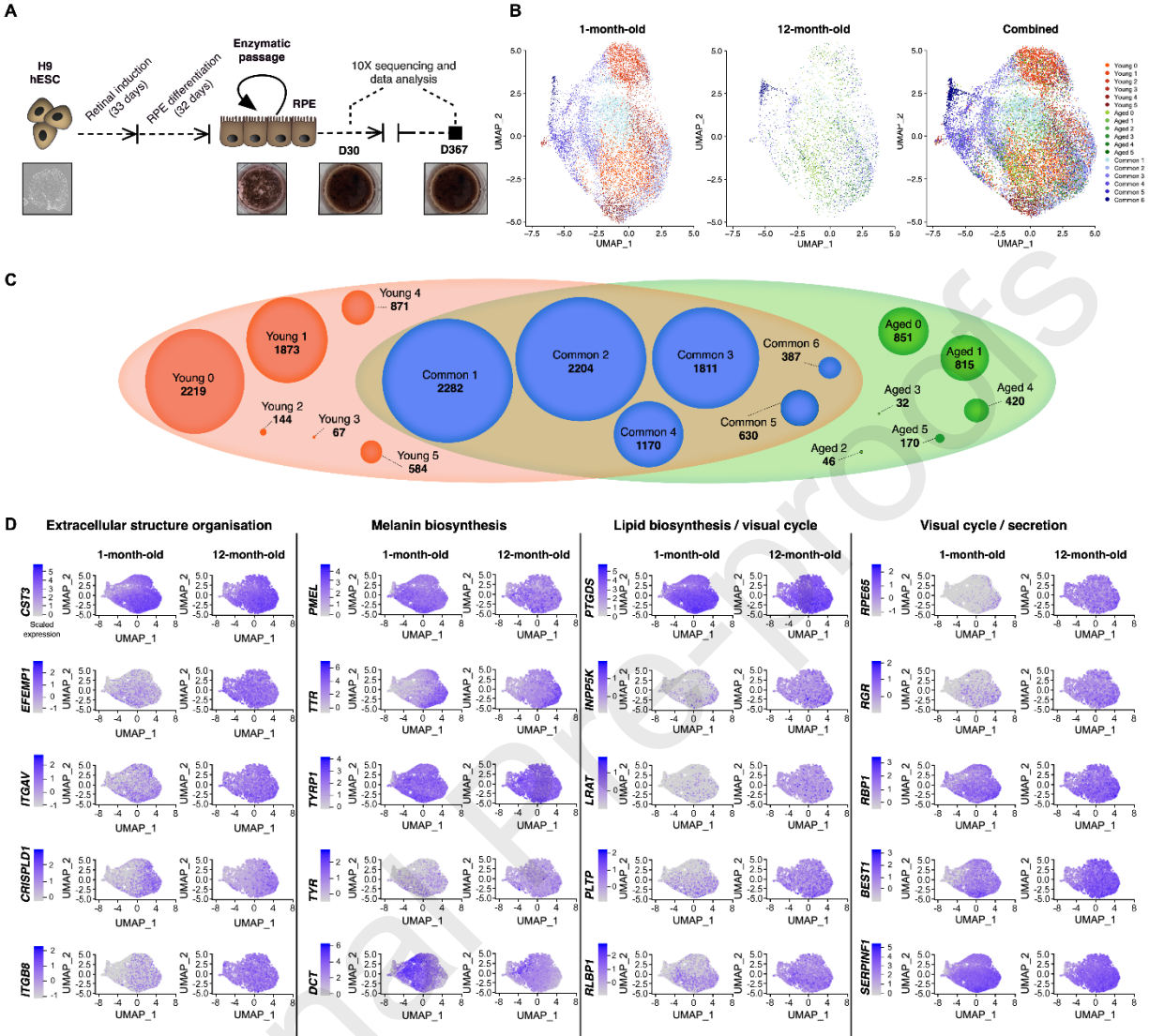
1161 Erica L. Fletcher, Shalin H. Naik: Conceptualization; Methodology; Funding acquisition; Roles/
1162 Writing - review & editing.

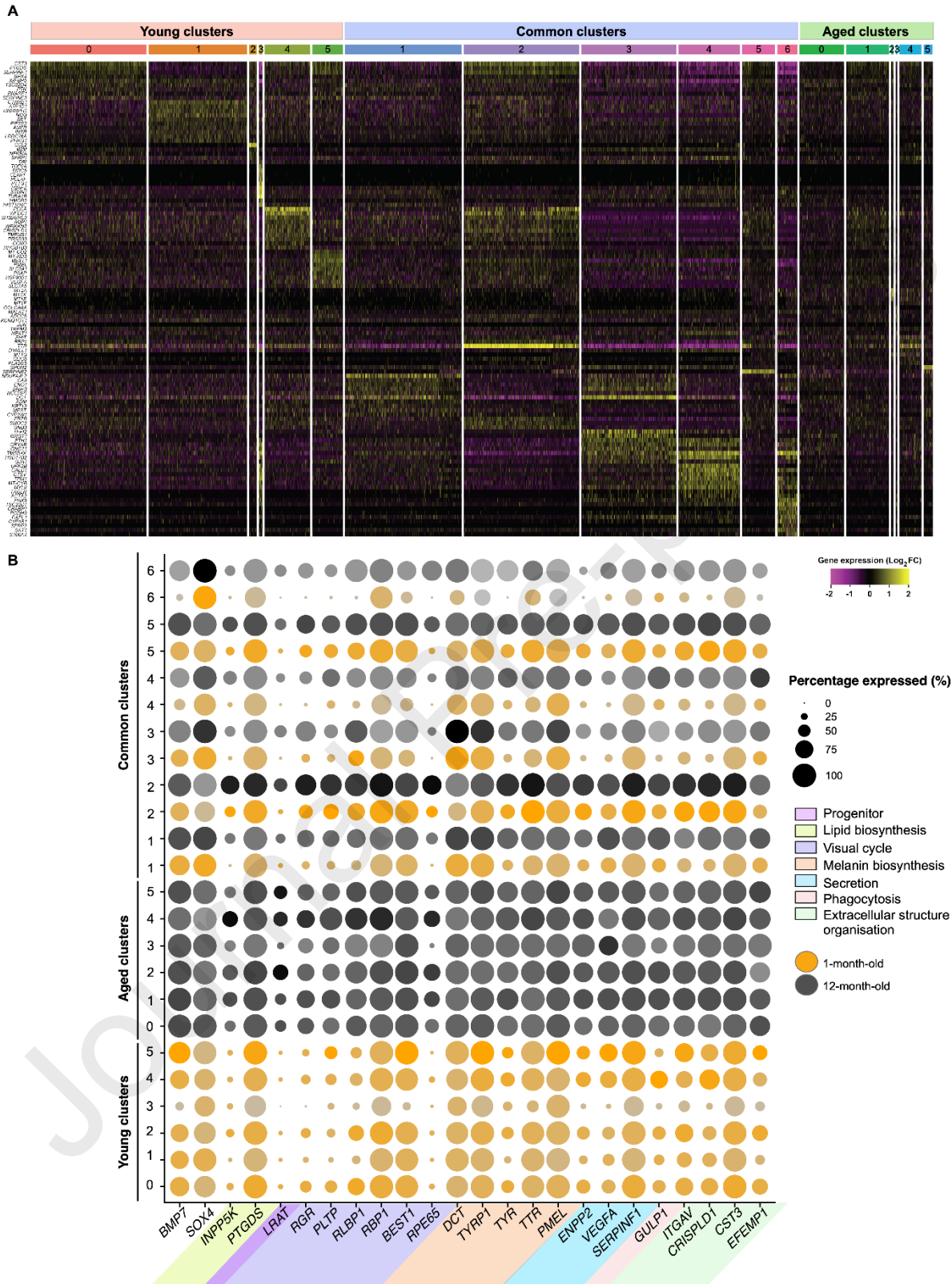
1163 Alex W. Hewitt: Conceptualization; Funding acquisition; Methodology; Resources; Writing -
1164 review & editing, Supervision

1165 Joseph E. Powell: Conceptualization; Data curation; Formal analysis; Funding acquisition;
1166 Methodology; Resources; Software, Roles/Writing - original draft; Writing - review & editing,
1167 Supervision

1168 Alice Pébay: Conceptualization; Formal analysis; Visualization; Funding acquisition;
1169 Methodology; Project administration; Resources; Roles/Writing - original draft; Writing - review
1170 & editing, Supervision.

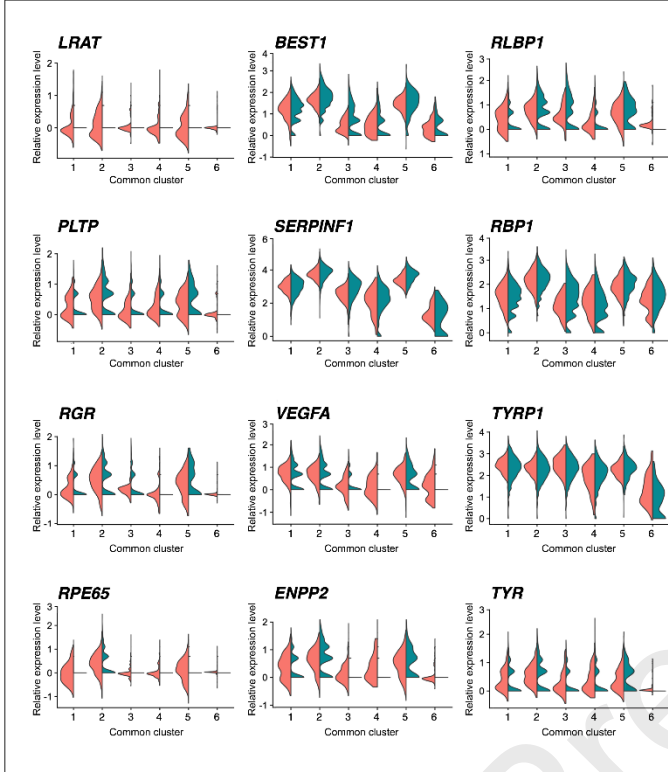
1171



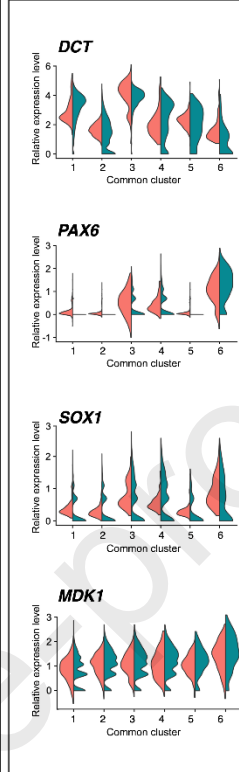


1173

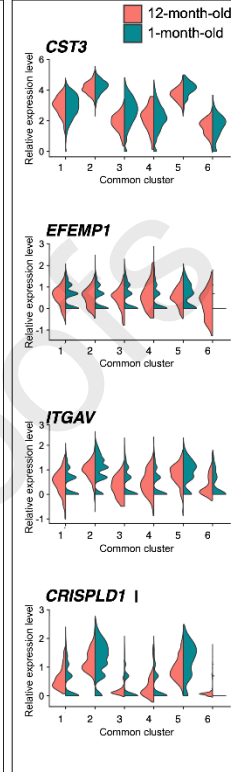
A RPE marker



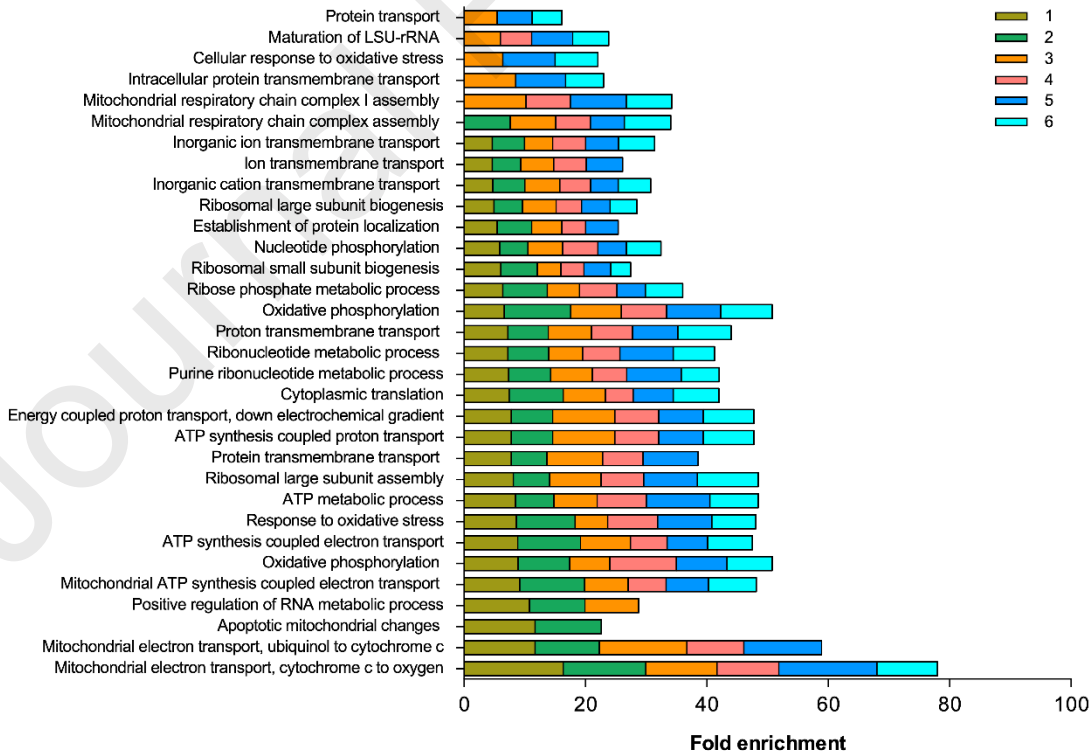
B Neural differentiation marker

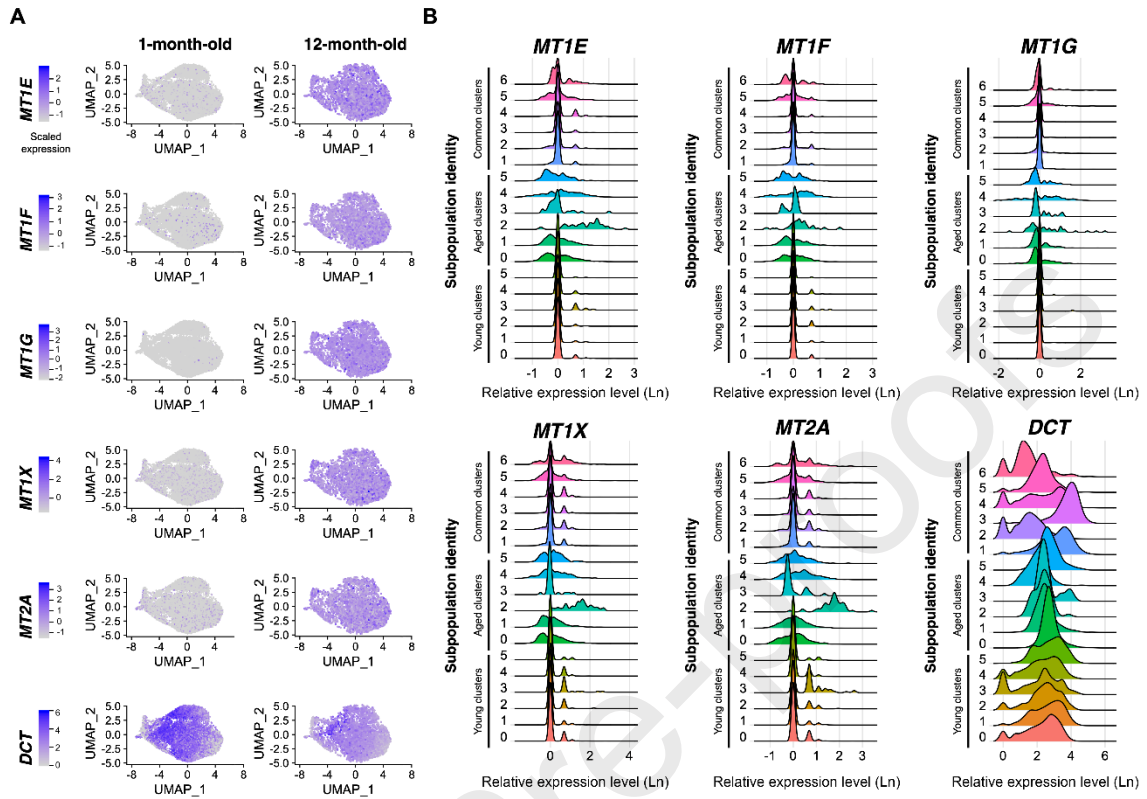


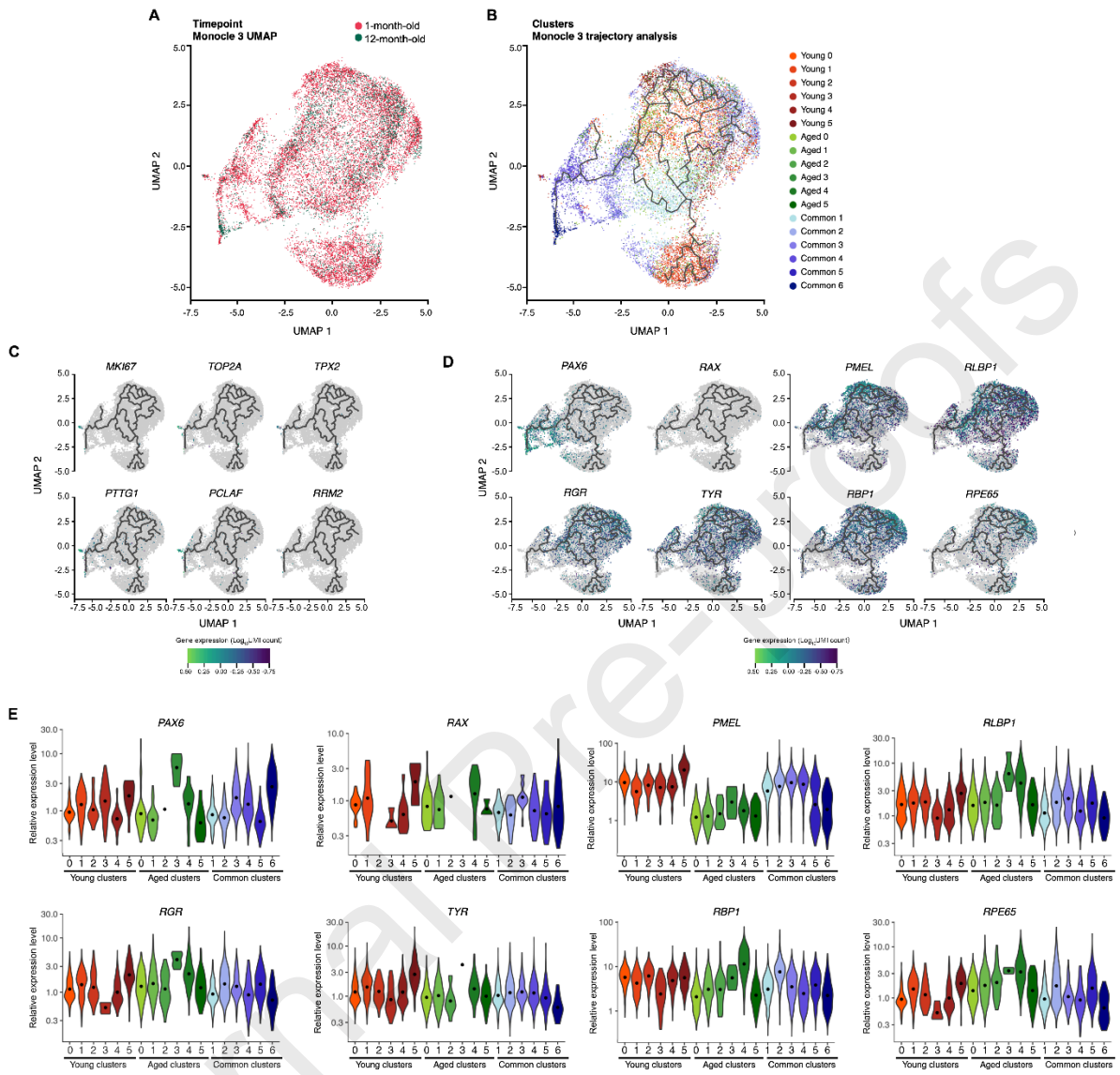
C ECM marker

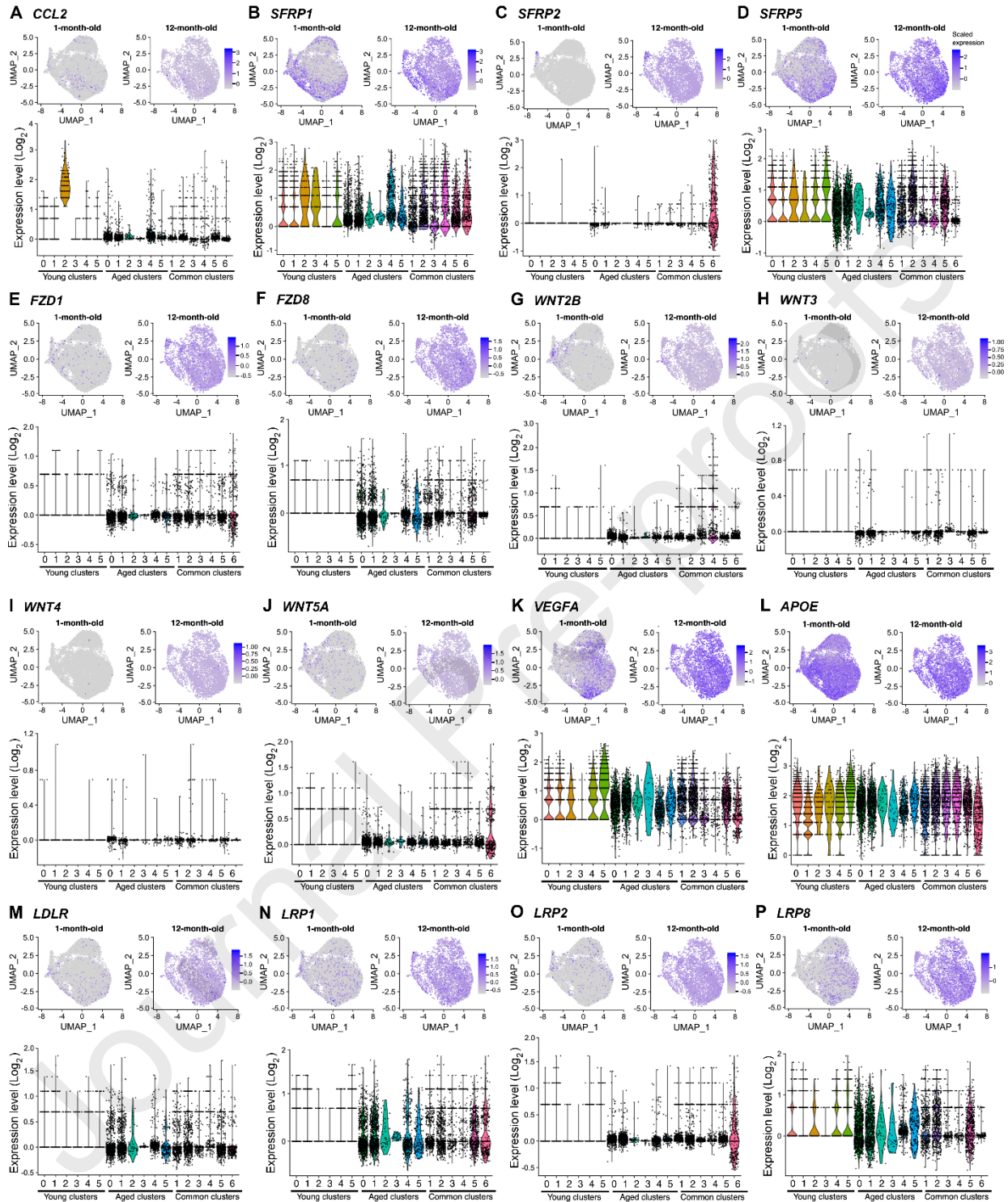


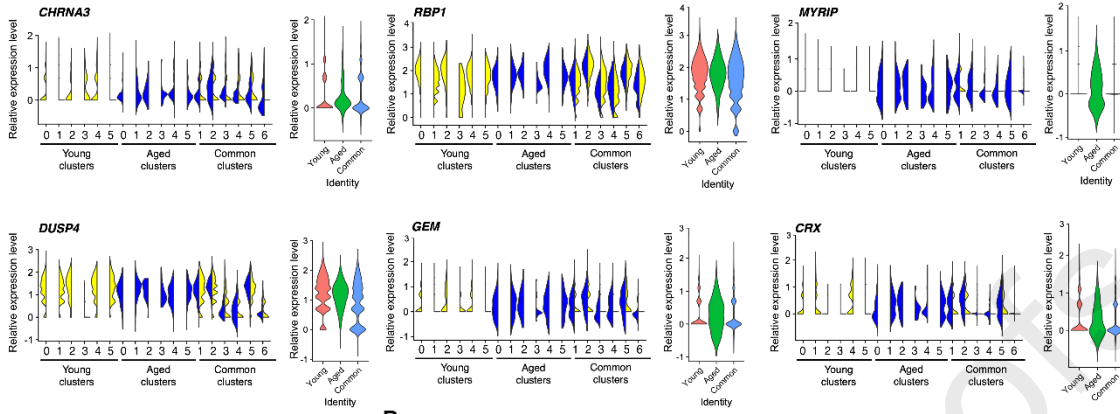
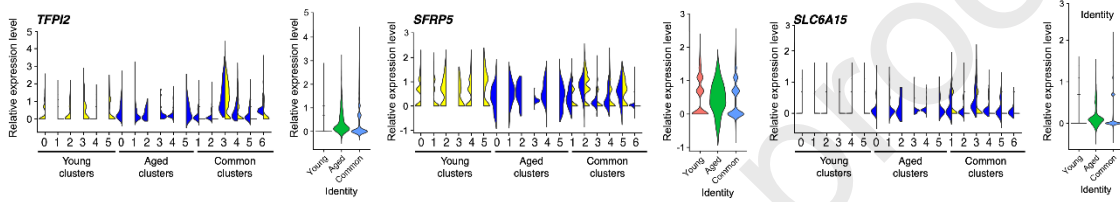
D GO-slim biological process

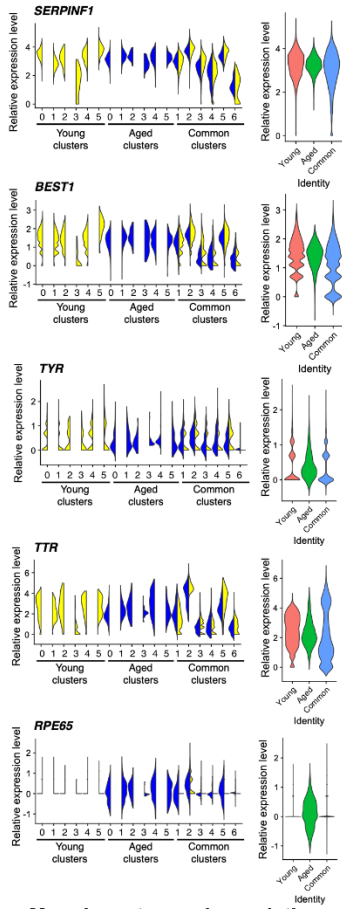
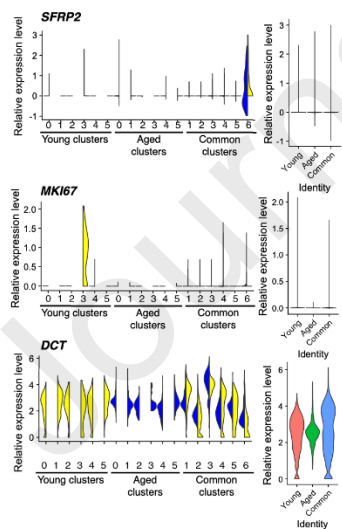
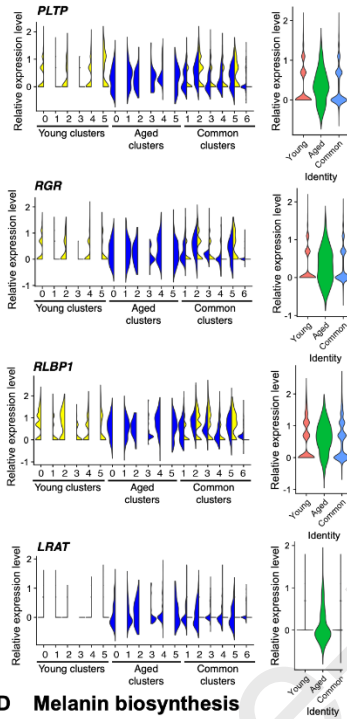
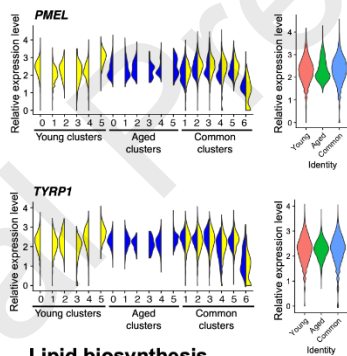
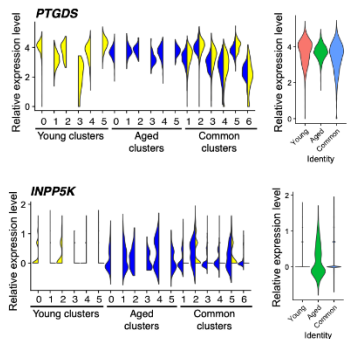
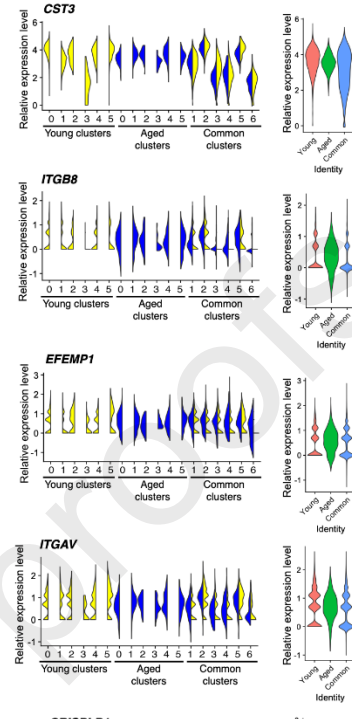
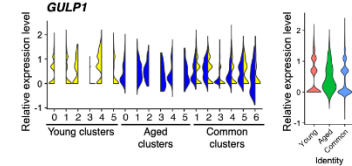








A Upregulated in adult RPE**B Downregulated in adult RPE**

A All subpopulations**B More immature subpopulations****C Visual cycle****D Melanin biosynthesis****E Lipid biosynthesis****F Extracellular structure organisation****G Phagocytic activity****H Secretion**